Published in final edited form as:
Dev Biol. 2010 August 15; 344(2): 621–636. doi:10.1016/j.ydbio.2010.05.497.

Characterization of a dominant-active STAT that promotes tumorigenesis in *Drosophila*

Laura A. Ekas, **Timothy J. Cardozo**, **Maria Sol Flaherty**, **Elizabeth A. McMillan**, **Foster C. Gonsalves**, and **Erika A. Bach***
Pharmacology Department, New York University School of Medicine, New York, New York 10016-6402, USA

Abstract

Little is known about the molecular mechanisms by which STAT proteins promote tumorigenesis. *Drosophila* is an ideal system for investigating this issue, as there is a single STAT (Stat92E), and its hyperactivation causes overgrowths resembling human tumors. Here we report the first identification of a dominant-active Stat92E protein, Stat92E$^{\Delta N\Delta C}$, which lacks both N- and C-termini. Mis-expression of Stat92E$^{\Delta N\Delta C}$ *in vivo* causes melanotic tumors, while *in vitro* it transactivates a *Stat92E-luciferase* reporter in the absence of stimulation. These gain-of-function phenotypes require phosphorylation of Y^{711} and dimer formation with full-length Stat92E. Furthermore, a single point mutation, an R^{442P} substitution in the DNA-binding domain, abolishes Stat92E function. Recombinant Stat92E^{R442P} translocates to the nucleus following activation but fails to function in all assays tested. Interestingly, R^{442} is conserved in most STATs in higher organisms, suggesting conservation of function. Modeling of Stat92E indicates that R^{442} may contact the minor groove of DNA via invariant TC bases in the consensus binding element bound by all STAT proteins. We conclude that the N- and C- termini function unexpectedly in negatively regulating Stat92E activity, possibly by decreasing dimer dephosphorylation or increasing stability of DNA interaction, and that Stat92E^{R442} has a nuclear function by altering dimer:DNA binding.

Keywords

STAT; JAK; Unpaired; *Drosophila*; constitutively active; in vitro reporter; in vivo reporter; structure function; signal transduction

Introduction

The Janus Kinase/Signal Transducer and Activator of Transcription (JAK/STAT) pathway is evolutionarily conserved and is critical for numerous biological processes, including immunity and proliferation (reviewed in (Arbouzova and Zeidler, 2006; Levy and Darnell, 2002)). STATs are a family of latent cytoslic transcription factors that are activated by tyrosine phosphorylation, which allows the formation of an activated dimer through reciprocal phosphorylated tyrosine-Src Homology 2 (SH2) interactions between two STAT monomers. Studies in cultured cells have led to a model in which JAK non-receptor tyrosine

* Corresponding author: Erika A. Bach, Pharmacology Department, New York University School of Medicine, 550 First Avenue, MSB 497B, New York, NY 10016-6402 USA, Tel: +1 (212) 263-5963, FAX: +1 (212) 263-7133, erika.bach@nyu.edu.

The authors state no conflict of interests.

kinases, constitutively associated with transmembrane receptors, are activated following ligand binding (Fig. 1A). JAK activation leads to the subsequent tyrosine phosphorylation of receptor sites to which unphosphorylated STAT dimers dock. STAT dimers are activated by JAK-dependent tyrosine phosophorylation and are then able to bind to consensus sequences in target genes and influence their transcription (Becker et al., 1998; Braunstein et al., 2003; Chen et al., 2003; Chen et al., 1998; Kretzschmar et al., 2004; Mao et al., 2005; Neculai et al., 2005; Novak et al., 1998; Schroder et al., 2004; Stancato et al., 1996). The activity of phosphorylated STAT dimers is transient, and these dimers are dephosphorylated in the nucleus and are exported to the cytoplasm (Mertens et al., 2006; Reich and Liu, 2006; Zhong et al., 2005).

Mammals have seven STAT proteins (STAT1-4, 5a, 5b, and 6) that share a similar a conserved domain structure, including N-terminus, coiled-coil, DNA-binding, linker, SH2, and C-terminus (Fig. 1B and (Becker et al., 1998;Chen et al., 1998;Vinkemeier et al., 1998)). The N-terminal domain (residues ~1-130) is required for formation of tetramers as well as of non-phosphorylated dimers, for tyrosine dephosphorylation, for transcriptional activation and for protein-protein interactions (Chang et al., 2003;Chen et al., 2003;Murphy et al., 2000;Ota et al., 2004;Shuai et al., 1996;Vinkemeier et al., 1998;Xu et al., 1996). A helical coiled-coil domain beginning around residue 130 mediates interaction between several proteins including c-Jun (Zhang et al., 1999). The DNA-binding domain of STATs (DBD) (residues ~320 to 490) has limited contact with both the major and minor grooves of DNA (Chen et al., 1998). The linker domain (residues ~490 to 580) modulates the rate of STAT:DNA interactions, ultimately controlling transcriptional activation of STAT target genes (Yang et al., 2002). An SH2 domain (residues ~580-680) is required for the formation of an activated STAT dimer by mediating reciprocal interactions with a phosphorylated conserved tyrosine residue at position ~700 that exists in all STATs (Chen et al., 1998;Levy and Darnell, 2002). The phosphorylation of this tyrosine residue is required for STAT function, which is abolished by its mutation to Phe in all species tested (Levy and Darnell, 2002). Lastly, the carboxy-terminal transactivation domain (TAD) varies in length from 38 to 200 amino acids interacts and is required for transcriptional co-activation of mammalian STATs (Horvath, 2000).

Gain-of-function mutations in the *Drosophila* JAK *hopscotch* (*hop*) were the first to link the JAK/STAT pathway to cancer. These *hop* alleles result in hyperactive kinases that cause an over-proliferation of blood cells, leading to fly “leukemia” and lethality (Binari and Perrimon, 1994; Hanratty and Dearolf, 1993; Harrison et al., 1995; Luo et al., 1995). Similarly, sustained activation of the JAK/STAT pathway is a causal event in human leukemia and myeloproliferative disorders (Baxter et al., 2005; James et al., 2005; Jones et al., 2009; Kilpivaara et al., 2009; Lacronique et al., 1997; Levine et al., 2005; Olcaydu et al., 2009). Persistent activation of Stat3 is associated with a dozen types of human cancer, including all classes of carcinoma (Darnell, 2005). Moreover, a dominant-active form of Stat3, called Stat3-C, generated by conversion of two residues in the C-terminal loops of the SH2 domain to Cys, is oncogenic and causes tumors in nude mice (Bromberg et al., 1999). The constitutive transcriptional abilities of Stat3-C require tyrosine phosphorylation of Y^{705} and likely arise because the cysteine mutations increase occupancy of the STAT dimer on DNA and/or prevent its dephosphorylation, which results in the accumulation of activated STAT dimers (Li and Shaw, 2006; Liddle et al., 2006). Inhibition of Stat3 arrests the growth of primary human cancer cells, which makes Stat3 an attractive target for cancer therapy (Blaskovich et al., 2003; Chiarle et al., 2005; Song et al., 2005; Sun et al., 2005).

Redundancy in components of the mammalian JAK/STAT pathway exists at each level of this signaling cascade. In contrast, the *Drosophila* pathway is a complete yet simplified version of its mammalian counterpart (Arbouzova and Zeidler, 2006). Three related IL-6-

like cytokines, Unpaired (Upd), Upd2 and Upd3, activate a gp-130-like receptor Domeless (Dome), which leads to the activation of the sole JAK Hop and the sole STAT Stat92E (Fig. 1A and (Agaisse et al., 2003; Binari and Perrimon, 1994; Brown et al., 2001; Chen et al., 2002; Gilbert et al., 2005; Harrison et al., 1998; Hombria et al., 2005; Hou et al., 1996; Sefton et al., 2000; Yan et al., 1996)). Activated Stat92E regulates expression of target genes, such as *Socs36E*, which encodes a negative regulator of the pathway (Callus and Mathey-Prevot, 2002; Issigonis et al., 2009; Karsten et al., 2002; Rawlings et al., 2004). This pathway plays important roles in many aspects of *Drosophila* development, including embryonic and eye development and larval hematopoiesis (reviewed in (Arbouzova and Zeidler, 2006)). Sustained JAK/STAT signaling in the fly eye during development leads to an enlarged eye that is 2-3 times larger than wild type (Bach et al., 2003; Juni et al., 1996; Tsai and Sun, 2004). Furthermore, loss of tumor suppressor genes *tsg-101* and *vps25* lead to excessive activation of JAK/STAT pathway signaling and over-growth of the eye, and this phenotype is suppressed by removal of one copy of *Stat92E* (Herz et al., 2006; Moberg et al., 2005; Thompson et al., 2005; Vaccari and Bilder, 2005). In contrast, global loss of *Stat92E* during eye development leads to an ablated eye and lethality prior to adulthood (Ekas et al., 2006; Hou et al., 1996; Tsai et al., 2007; Yan et al., 1996).

Stat92E is a 761 amino acid protein that shares a similar domain structure to other STATs and that is most similar to human STAT5 with 37% identity (Hou et al., 1996; Yan et al., 1996; Zeidler et al., 2000). Despite the sequence similarity between mammalian STATs and Stat92E, the functional requirements of the different domains in Stat92E are largely unknown, and an in-depth structural analysis of this protein has not been undertaken. To address this issue, we designed *in vivo* rescue assays and *in vitro* readouts to investigate the role of the N- and C-terminal domains in Stat92E. We also examined the requirement of Arg^{442}, which is conserved in the majority of mammalian STATs, and is mutated to Pro in the strong hypomorphic allele $Stat92E^{85C9}$ (Silver and Montell, 2001; Wang and Levy, 2006a). Surprisingly, we found that neither the first 133 nor the last 36 amino acids are required for Stat92E function. Furthermore, removal of both of these domains simultaneously resulted in a constitutively active form of Stat92E, the oncogenic activity of which depends on phosphorylation of Y^{711}. We also demonstrated that Arg^{442} is required for Stat92E function, presumably because it forms a key STAT:DNA contact point.

Materials and Methods

Genetics

These stocks are described in FlyBase: $Stat92E^{85C9}$; $Stat92E^{397}$; $Stat92E^{06346}$; $Stat92E^{j6C8}$; *outstretched* (*os*); *UAS-upd; UAS-hop; tub-Gal4; Df(3R)H-B79; UAS-GFP; ey-Gal4* (Hauck et al., 1999); *P[AyGAL4]25 P[UAS-GFP.S65T]T2; hs-flp MKRS/TM6B; ey-Gal4, UAS-flp* (Stowers and Schwarz, 1999); *M(3)96C; Ribosomal protein S3* (*RpS3*)^1; and FRT^{82B} ry^{506}. We also used *10×STAT-GFP* (Bach et al., 2007). *actin-Gal425/CyO* was a gift of Norbert Perrimon. Crosses were maintained at 25°C.

We used the Mosaic Analysis with a Repressible Cell Marker (MARCM) technique to generate positively-marked $Stat92E^{85C9}$ clones that over-expressed $Stat92E^{\Delta N \Delta C}$ (Lee and Luo, 1999).

For the MARCM analyses, we crossed *w; UAST-3HA-*$Stat92E^{\Delta N \Delta C}$*/UAST-3HA-*$Stat92E^{\Delta N \Delta C}$*;* FRT^{82B} *Stat92E/TM6C,Tb,Sb* flies to *ey-flp, UAS-GFP; tub-Gal4/CyO;* FRT^{82B} *tub-Gal80/TM6B,Tb* or *hs-flp, UAS-GFP 6xMyc, tub-Gal4*; +/+; FRT^{82B} *tub-Gal80/TM6B,Tb*.

In animals possessing the *ey-Gal4, UAS-flp* (EGUF (Stowers and Schwarz, 1999)) chromosome, the *ey* promoter drives expression of the yeast Gal4 transactivator from the earliest stages of eye development (Stowers and Schwarz, 1999). Gal4 stimulates the expression of genes under the control of *Upstream Activating Sequences* (*UAS*) via the UAS/Gal4 technique (Brand and Perrimon, 1993). In this case, Gal4 induces *flp*, and FLP induces mitotic recombinantion between homologous *Flippase Recognition Target* (*FRT*) sites by means of the FLP/FRT technique (Xu and Rubin, 1993). *Minutes* are mutations in ribosomal genes that cause slow growth and recessive lethality in cells possessing the wild type chromosome, providing a growth advantage to the homozygous (*e.g., Stat92E*) tissue (Lambertsson, 1998; Morata and Ripoll, 1975). *Minute* clones were made using FRT^{82B} *M(3)96C, arm-lacZ* or FRT^{82B} $RpS3^{1}$, *ubi-GFP* stocks. FRT^{82B} ry^{506} was used as the control + chromosome. When *EGUF* flies also carry a *UAS-3HA-Stat92E* transgene, *ey-Gal4* drives expression of both *UAS-flp* and *UAS-3HA-Stat92E* in the eye disc. This results in the generation of homozygous *Stat92E* mutant tissue and the expression of 3HA-Stat92E proteins specifically in eye disc cells.

Clones mis-expressing *hop* and $Stat92E^{\Delta N \Delta C}$ were generated by crossing *UAS-hop* or *UAS-*$Stat92E^{\Delta N \Delta C}$ flies with *P[AyGAL4]25 P[UAS-GFP.S65T]T2; hs-flp MKRS/TM6B* flies, in which FLP is under the control of the heat-shock promoter (Ito et al., 1997).

Transgene generation

Constructs

UASp-3HA-$Stat92E^{FL}$ (Ekas et al., 2006)

UASp-3HA-$Stat92E^{\Delta N}$

UASp-3HA-$Stat92E^{\Delta C}$

UASp-3HA-$Stat92E^{\Delta N \Delta C}$

UAST-3HA-$Stat92E^{\Delta N \Delta C Y711F}$

UAST-3HA-$Stat92E^{Y711F}$

UASp-3HA-$Stat92E^{R442P}$

UAST-3HA-$Stat92E^{R442K}$

UASp-3HA-$Stat92E^{R442A}$

Ac5c-hop-myc-his

socs1-luc

Primers

***Stat92E*$^{\Delta N}$**

5′DELTA1-133

5′ TTTTTGGATCCATGAACAACACGCCCATGGTTACCGGG 3′

3′DELTA1-133

5′ GTTGGTGGCGCCAGTTCTTGAGCTCG 3′

***Stat92E*$^{\Delta C}$**

5′delta725-761

5′ CAGATCCGTGTGTGGACCCTGTCCTTAC 3′

3′delta725-761

5′ TTTTGCGGCCGCTCCGTTTCTACAAACGTGAACATGCAATG 3′

Stat92E$^{\Delta N \Delta C Y711F}$

5′ Primer

5′ CTCGTCCTAGATCCTGTGACCGGTTTTGTGAAGAGCACATTGCATGTTCAC 3′

3′ Primer

5′ GTGAACATGCAATGTGCTCTTCACAAAACCGGTCACAGGATCTAGGACGAG 3′

Stat92E^{Y711F}

5′ B YF NEW

.5′ GTTCTAGATCCTGTGACCGGTTTTGTGAAGAGCACATTGCATGTTCAC 3′

3′ B YF NEW

5′ GGGCTATGCGGCCGCAAAGTTCTCAAAGTTTGTAATCGTATC 3′

Stat92E^{R442P}

5′R442PB

5′ GCCCTTCTTTTCTGCCGGCTTGATCTTCTTCAG 3′

3′R422PA

5′ CTGAAGAAGATCAAGCCGGCAGAAAAGAAGGGC 3′

Stat92E^{R442K}

5′R442K B

5′ CTGAAGAAGATCAAGAAGGCAGAAAAGAAGGGC 3′

3′R442K A

5′ GCCCTTCTTTTCTGCCTTCTTGATCTTCTTCAG 3′

Stat92E^{R442A}

5′ R442A B

5′ CTGAAGAAGATCAAGGCGGCAGAAAAGAAGGGC 3′

3′ R442A A

5′ GCCCTTCTTTTCTGCCGCCTTGATCTTCTTCAG 3′

Ac5c-hop-myc-his

5′ Oligo (Oligo 37)

5′ GAGTATCTGCAATCTGGTTCCTTCGAC 3′

3′ Oligo (Oligo 38) (to put an *Xba*I site at 3′ end of *hop* cDNA and subclone in frame with Myc and His tags)

5′ GGAAATCTAGAAACTCGGCATCCGTCGGCTGATTCGGCGGCGAC 3′

socs1-luc

5′ Oligo

5′-TTTTTAGATCTGACTGTTTACCGCTTGCGGGTCGCATTTC-3′ (*Bgl*II site)

3′ Oligo

5′-TTTTTGGATCCCCTTAACAACTGGCTTGAACTTATGTTTA-3′ (*Bam*HI site).

Transgene generation

A full-length *Stat92E* cDNA containing three N-terminal HA tags was ligated into *UASp* to generate the *UASp-3HA-Stat92E*^{FL} transgene as described in (Ekas et al., 2006). We have subsequently discovered that *3HA-Stat92E*^{FL} transgene has a silent point mutation that results in an Ala substitution of Ser at position 8. This mutation does not effect the function of the 3HA-Stat92E^{FL} protein since it can rescue *Stat92E* loss-of-function phenotypes ((Ayala-Camargo et al., 2007; Ekas et al., 2006), this study and data not shown). The constructs in this study were engineered by polymerase chain reaction (PCR) using the primers above and the *C5HA3-3HA-Stat92E*^{FL} plasmid as a template. *C5HA3* is a *pBluescript KS*-based vector *C5HA3* (Nybakken et al., 2005). The 5′ end of the *C5HA3* polylinker includes an ATG immediately upstream of sequence encoding three HA epitopes, followed by an in-frame *Bam*HI site. At the 3′ end, a *Not*I site immediately precedes and is in frame with a stop codon. All *Stat92E* constructs in this study were designed to have *Bam*HI (5′) and *Not*I (3′) ends. After digestion with *Bam*HI and *Not*I, the insert was ligated into *C5HA3* that had also been digested with *Bam*HI and *Not*I. For the *3HA-Stat92E*$^{\Delta N}$, *3HA-Stat92E*$^{\Delta C}$ and *3HA-Stat92E*^{R442P} plasmids, the insert was excised from *C5HA3* by digestion with *Bss*HII. The 3′ recessed termini were filled in with Klenow and were ligated into *UASp* (Rorth, 1996) that had been cut with *Bam*HI, filled in Klenow and treated with Shrimp Alkaline Phosphatase (SAP) (Roche). For *3HA-Stat92E*$^{\Delta N\Delta C}$, a ~400 bp fragment deleting the first 133 amino acids was generated by PCR using the primers for the *3HA-Stat92E*$^{\Delta N}$ construct. This fragment was digested with *Bam*HI and *ClaI* and ligated into the *C5HA3-3HA-Stat92E*$^{\Delta C}$ vector that had been digested with *Bam*HI and *Cla*I. It was subsequently cloned into *UASp* as described above For *3HA-Stat92E*$^{\Delta N\Delta CY711F}$, *3HA-Stat92E*^{R442K}, *3HA-Stat92E*^{R442A}, and *3HA-Stat92E*^{Y711F}, oligos containing an *Avr*II restriction site were made to the 5′ and 3′ ends of the *Stat92E* transgenes and PCR was then used to remove the entire transgenic sequence (including the 3 HA tags). Inserts were cut with *Avr*II and ligated into *UAST* (Brand and Perrimon, 1993) that had been cut with *XbaI* and treated with SAP. Throughout the text, these constructs are frequently referred to without the "*UAS*" preface. Transgenic lines were by injection into *w*^{1118} *Drosophila* embryos (CBRC Transgenic Fly Core, Charlestown, MA). Multiple insertions of each *UAS-3HA-Stat92E* transgene were tested in each assay, and similar results were obtained for each construct.

To make the *Ac5c-hop-myc-his* construct, we subcloned the entire ~5 kb *Apa*I-*Xba*I fragment of the *hop* cDNA from *Bluescript-hop* (Binari and Perrimon, 1994) into *pcDNA3.1(-)/myc-His B* (Invitrogen). The resulting plasmid was called *pcDNA3.1-hop-myc-His-ApaI-XbaI*. The parental *pcDNA3.1(-)/myc-His B* plasmid contains C-terminal Myc and His epitodes tags followed by a stop codon and preceded by unique restriction enzyme sites. To remove the stop coding from the *pcDNA3.1-hop-myc-His-ApaI-XbaI* plasmid, we amplified by PCR a 600 bp fragment of the C-terminal end of *hop* and mutated the stop codon, inserted an *XbaI* site and engineered it to be in frame with the Myc and His tags. This fragment was digested with *Pfl*MI (a unique site in *hop*) and *Xba*I and the resulting 355 bp band was purified and ligated into the *pcDNA3.1-hop-myc-His-ApaI-XbaI* plasmid vector at the *Pfl*MI and *Xba*I sites. The resulting plasmid *pcDNA3.1-hop-myc-his* was cut with *Not*I and *Pme*I, which removes 500 bp of the 5′UTR of the *hop* cDNA but leaves the start site, the epitopes tags, stop codon intact. The *Not*I-*Pme*I fragment was treated with SAP and

subcloned into the *Actin5c* (*Ac5c*) plasmid that had been digested with *Not*I and *Hpa*I and treated with SAP. The construct was verified by sequencing and by Western blotting (data not shown). In the text describing in the *in vitro* transfection assays, “Hop-Myc-His” is also referred to as “Hop”.

To generate the *socs1-luc* reporter we used PCR to amplify an 862 bp fragment of genomic *Socs36E* intron 1 DNA from isogenized FRT^{42} flies (Janody et al., 2004) with *Bgl*II (5′) and *Bam*HI (3′) ends. After digestion with *Bgl*II and *Bam*HI, the insert was ligated into a *pGL3* Basic Vector (Promega) at the *Bgl*II site. *socs1-luc* was excised from *pGL3* at *Sma*I and *Xba*I sites and ligated in *pCaSpeR 4* at *Spe*I and *Xba*I sites.

in situ hybridization and antibody staining

in situ hybridization and antibody stainings were performed as described in (Bach et al., 2003; Flaherty et al., 2009). We used mouse anti-Discs large (Dlg) (1:50) (Developmental Hybridoma Studies Bank (DHSB)); rabbit anti-β-galactosidase (1:100) (Cappel); rat anti-HA (1:1000) (clone 3F10, Roche); 4′,6-diamidino-2-phenylindole (DAPI) (1:1000) (Invitrogen); rabbit anti-Stat92E (1:1000) (Flaherty et al., in press) and fluorescent secondary antibodies at 1:250 (Jackson Laboratories). Fluorescent images were taken of eye discs (at 25×) using a Zeiss LSM 510 confocal microscope and of cells (at 40×) using a Nikon Eclipse TE2000-E microscope and digital camera. Bright field pictures were taken at 5× using a Leica MZ 8 microscope with an Optronics digital camera or at 20× using a Zeiss Axioplan microscope with a Nikon Digital Sight DL-UL camera.

Western blot analysis

Extracts from S2 cells were prepared by lysis in a buffer containing 1×PBS, 150 mM NaCl, 1% Triton, 1× Complete protease inhibitors (Roche), 2 mM sodium orthovanadate, and 0.5 mM EDTA. Immunoprecipitation was performed as described in (Bach et al., 1996) using rat anti-HA (1:1000) (clone 3F10, Roche) and Protein A-Sepharose (Amersham Biosciences). Immunoprecipitated proteins were eluded, subjected to SDS-PAGE and immunoblotted using standard methods. We used PY-20 (1:1000) (BD Biosciences); mouse anti-HA (1:000) (Covance); and rabbit anti-Stat92E (1:1000) (Flaherty et al., in press). Horseradish peroxidase secondary antibodies (Jackson ImmunoResearch) were used (1:10,000). The blots were developed using Amersham ECL Western Blotting Analysis System (GE Healthcare).

Luciferase assay

Luciferase assays were performed as described in (DasGupta et al., 2005). 6×10^4 S2 cells were seeded in 96-well plates and transfected using Effectene (Qiagen) with 40 ng of *Ac5c-Gal4* (Zeidler et al., 2004), 40 ng of *UAS-3HA-Stat92E* transgene, 40 ng of *socs1-luc*, 40 ng of Renilla-luciferase and 4 ng of *Ac5c-hop-myc-his*. *Ac5c* was added as needed to maintain a constant concentration of DNA. After 48 hours, firefly luciferase (from *socs1-luc*) and Renilla luciferase activity were monitored in cell lysates using Dual-Glo Luciferase Assay System (Promega) and a Perkin Elmer Wallac EnVision 2103 multilabel plate reader. Experiments were performed four times in quadruplicate. For each data point, firefly luciferase values were divided by appropriate Renilla luciferase value. Relative luciferase units were then calculated by Nexperimental/Nconstant where Nexperimental is the value of firefly luciferase/Renilla luciferase and Nconstant is Ac-Gal4 firefly luciferase/Renilla Luciferase.

Stat92E homology model

The homology model was built as described in (Cardozo et al., 1995) using the ICM-Pro software program (Molsoft, LLC, La Jolla, CA). Briefly, the crystal structure of phosphorylated STAT1 was used as a template (pdb code 1bf5) for the sequence of Stat92E (Q24151). The similarity between the sequence of the template and the sequence of Stat92E is high enough to virtually guarantee that Stat92E adopts the same overall 3D fold as the template. After threading the Stat92E sequence onto the STAT1 crystal structure using the alignment between the two sequences as a guide, side-chains and loops were energy minimized to obtain the final 3D structural model.

Alignments

Protein sequences were obtained from NCBI. The DNA binding domains were aligned by the Clustral-W method using DS Gene 1.5 software. Optimal STAT binding elements used in this study were originally reported in (Decker et al., 1997; Wang and Levy, 2006b; Yan et al., 1996).

Results

Generation of *UAS-3HA-Stat92E* transgenes

We previously reported the generation of a full length *Stat92E* transgene *UAS-3HA-Stat92E^{FL}*, which encodes the 761 amino acid Stat92E protein tagged at the N-terminus by 3 tandem HA epitopes (Ekas et al., 2006). This transgene fully rescues *Stat92E* phenotypes in the developing *Drosophila* eye (Fig. 3D and (Ekas et al., 2006)). To determine the functionally important sequences in Stat92E, we made deletions and substitutions to the *3HA-Stat92E^{FL}* construct and then assessed their performance in several assays (Fig. 1B).

Stat92E allelic series

First, we determined the *Stat92E* mutant background in which the *in vivo* experiments should be performed. We used lethal-phase analysis to assess the strongest *Stat92E* loss-of-function allele. The *Stat92E^{85C9}* and *Stat92E^{397}* are ethyl methanesulfonate-induced alleles that are caused by a substitution of Arg at position 442 to a Pro and of a Trp to a stop codon at position 594, respectively (Silver and Montell, 2001). Both *Stat92E^{06346}* and *Stat92E^{j6C8}* have P-element insertions 5′ to the start site of the *Stat92E* gene, which presumably lower transcription of this gene (Hou et al., 1996; Spradling et al., 1999). While P-element mutations are typically hypomorhpic, *Stat92E^{06346}* has been reported to be a null (Henriksen et al., 2002; Hou et al., 1996; Mukherjee et al., 2005; Zeidler et al., 1999). However, the level of *Stat92E* mRNA or protein in this mutant has never been published. We monitored the zygotic lethal phase of these *Stat92E* alleles placed *in trans* to a chromosomal deficiency *Df(3R)H-B79* that removes the *Stat92E* gene. 30% of *Stat92E^{85C9}/Df*, 30% of *Stat92E^{397}/Df*, 22% of *Stat92E^{06346}/Df* and 24% of *Stat92E^{j6C8}/Df* animals died during embryogenesis. In all four crosses, the embryos that did hatch subsequently died in the first larval instar (Fig. 2A). These data indicate that *85C9* and *397* are stronger alleles than *06346* and *j6C8*. In support of this conclusion, we found that *Stat92E^{85C9}* or *Stat92E^{397}* clones in the eye-antennal, wing or leg disc generated significantly stronger phenotypes than *Stat92E^{06346}* or *Stat92E ^{j6C8}* clones ((Ayala-Camargo et al., 2007; Ekas et al., 2006) and data not shown). We propose this *Stat92E* allelic series, starting with the strongest: *85C9 = 397 > j6C8 >06346*.

Characterization of *Stat92E^{85C9}* and *Stat92E^{397}*

To further characterize the *85C9* and *397* alleles we established assays in the developing eye-antennal disc, which is derived from a primordial of ~50 progenitor cells and gives rise

to the adult eye, antenna and head capsule (Dominguez and Casares, 2005). In wildtype eye discs, activation of the JAK/STAT pathway promotes proliferation of these progenitor cells and formation of the eye field (Bach et al., 2003; Chao et al., 2004; Ekas et al., 2006; Reynolds-Kenneally and Mlodzik, 2005; Tsai and Sun, 2004). An eye-antennal disc composed of almost entirely homozygous *Stat92E* mutant tissue (hereafter referred to as *Stat92E* M^+) was generated using *ey-Gal4, UAS-flippase* (*flp*) (*EGUF*) and *Minute* techniques (see Materials and Methods). *Stat92E* mRNA was ubiquitously expressed in an eye disc from animals carrying a control wild type chromosome in an *EGUF Minute* background (referred to as +M^+) (Fig. 2B). It was also ubiquitously expressed in eye discs in *EGUF Stat92E*^{85C9} M^+ or *Stat92E*^{397} M^+ animals (Fig. 2C,D). These data indicate that *85C9* and *397* alleles are not RNA nulls. To determine whether *85C9* is a protein null, we stained *Stat92E* M^+ eye discs with an antibody that recognizes the last 15 amino acids of Stat92E, a region lacking in Stat92E^{397} (Chen et al., 2002; Flaherty et al., in press; Silver and Montell, 2001). As expected, in *Stat92E*^{397} M^+ eye discs, the Stat92E antibody staining specifically overlapped with heterozygous tissue, which have one wild type copy of *Stat92E* (Fig. 2F, arrow). In contrast, *Stat92E*^{85C9} M^+ eye discs exhibited ubiquitous Stat92E staining in homozygous mutant tissue and reduced expression in GFP-positive heterozygous tissue (Fig. 2E, arrow), demonstrating that this allele is not a protein null.

in vivo function of *Stat92E* variants

The majority of animals harboring *Stat92E8*^{5C9} M^+ or *Stat92E*^{397} M^+ clones generated by *EGUF* do not hatch from the pupal case and those that do eclose exhibit small or ablated eyes (Fig. 3B,C and (Ekas et al., 2006)). We designed a rescue assay that would generate eye disc cells which were homozygous mutant for *Stat92E* and also mis-expressed a recombinant 3HA-Stat92E protein (see Materials and Methods). Using this assay, we found that the phenotypes and hatching rate in *EGUF Stat92E*^{85C9} M^+ or *Stat92E*^{397} M^+ animals were completely rescued by the expression of *UAS-3HA-Stat92*^{FL} but not by an irrelevant *UAS-linked* gene (Fig. 3E and (Ekas et al., 2006)). Mis-expression of Stat92E$^{\Delta N}$, which lacks the first 133 amino acids, Stat92E$^{\Delta C}$, which lacks the last 36 amino acids (residues 726-761), or Stat92E$^{\Delta N\Delta C}$, which lacks both the first 133 and the last 36 amino acids, fully restored the size of the *Stat92E*^{85C9} M^+ eye to wild type size (Fig. 3G-I). In addition, all of the pupae in these crosses hatched from their pupal cases. By contrast, mis-expression of Stat92E^{Y711F} did not increase the size of the *Stat92E* M^+ small eye, confirming that Tyr^{711} is critical for Stat92E function *in vivo* as it is *in vitro* (Fig. 3F and (Yan et al., 1996)). We quantified the eye area of 20 females of each genotype, which confirms these qualitative results (Fig. S1). Importantly, all *UAS-3HA-Stat92E* variants gave identical results in the *Stat92E*^{397} background, indicating that *Stat92E*^{85C9} phenotypes are not due to an additional lethal mutation on the *85C9* chromosome (Fig. 3M-R and data not shown). All transgenes were expressed in the eye disc, although Y^{711F} (and non-functional R^{442} mutants, see below) had lower expression in *Stat92E* M^+ mutant tissue (Fig. S2,A-J). The reduced expression of HA in these discs might result from aberrations in eye field patterning and/or to ectopic expression of signaling molecules like the Wnt family member Wingless, which represses JAK/STAT signaling, and the Notch pathway ligand Serrate (Ayala-Camargo et al., 2007; Ekas et al., 2006; Flaherty et al., 2009; Tsai et al., 2007). Nevertheless, these data demonstrate that Tyr^{711}, but not the N-terminal 133 and/or the C-terminal 36 amino acids, are required for Stat92E function *in vivo*.

To confirm that the *in vivo* functionality of these variants is not specific to eye development, we tested the ability of the *Stat92E* variants to delay the *Stat92E*^{85C9} lethal phase. We used the UAS/Gal4 technique to mis-express *UAS-Stat92E* transgenes in a homozygous *Stat92E*^{85C9} background using *tubulin-Gal4* (*tub-Gal4*), which is ubiquitously expressed during all developmental stages (Brand and Perrimon, 1993). It should be noted that these

animals still have maternal *Stat92E* mRNAs. 30% of *85C9/85C9* homozygotes died during embryonic stages, the same value as *85C9/Df* (Fig. 2A,3S). Mis-expression of Stat92E^{FL} significantly delayed this lethal phase and the majority of animals died during pupal stages (Fig. 3S). Mis-expression of Stat92E$^{\Delta N}$, Stat92E$^{\Delta C}$ or Stat92E$^{\Delta N\Delta C}$ also delayed the lethal phase in a manner similar to Stat92E^{FL} (Fig. 3S). It is unclear why these transgenes did not rescue *Stat92E^{85C9}* homozyotes to adulthood because the pupae from these crosses appeared normal upon dissection (data not shown). Another constitutive driver (*actin-Gal4*) shifted the *85C9/85C9* lethal phase to late larval stages with mis-expressing Stat92E^{FL} (data not shown). These data suggest that these drivers are not strong enough during larval/pupal stages or do not target one or more critical tissues at sufficient levels to insure survival to adult stages. Stat92E^{Y711F} could not delay the lethal phase of *Stat92E^{85C9}* homozygous animals. Moreover, it had dominant negative effects as more than 95% of these animals died during embryonic stages (Fig. 3S). Importantly, all *UAS-3HA-Stat92E* variants gave identical results in *Stat92E^{397}* zygotic homozygotes (data not shown). These data suggest that the N- and C-terminal domains are not required for Stat92E function during all stages *of Drosophila* development, while Tyr^{711} is essential.

in vitro function of *Stat92E* variants

To investigate whether the 3HA-Stat92E variants can activate gene transcription *in vitro*, we generated a transcriptional reporter *socs1-luc* by placing an 880 bp fragment from intron 1 of the *Socs36E* gene containing four putative Stat92E binding sites upstream of *luciferase* (Bach et al., 2007; Baeg et al., 2005; Karsten et al., 2002). We transfected S2 cells with *Ac5c-hop-myc-his* that drives constitutive expression of Hop-Myc-His, with *Ac5c-Gal4* that induces *UAS* transgenes *in vitro* (Klueg et al., 2002), and with *UAS-3HA-Stat92E^{FL}*. We used 4 ng of *Ac5c-hop-myc-his*, which activated the reporter only slightly above the *Ac5c-Gal4* control (Fig. 4A, Lanes 1,2). Expression of Stat92E^{FL} alone did not activate the reporter above Hop-Myc-His control (Fig. 4A, Lane 3). By contrast, Stat92E^{FL} expressed together with Hop-Myc-His resulted in a signficant increase in luciferase activity (Fig. 4A, Lane 4).

We assessed which residues of Stat92E were required for the activation of *socs1-luc*. Stat92E$^{\Delta N}$ and Stat92E$^{\Delta C}$ robustly activated the reporter to levels observed with Stat92E^{FL} and only when expressed with Hop-Myc-His (Fig. 4A,B, Lanes 5,6). In contrast, Stat92E^{Y711F} could not activate the reporter *socs1-luc* when expressed alone or with Hop-Myc-His (Fig. 4A,B, Lanes 8). Western blotting demomstrated that all Stat92E constructs were expressed at similar levels and at the predicted M$_r$ (Fig. 4D). We further showed that all constructs were tyrosine phosphorylated after treatment of the cells with pervanadate, which activates Stat92E in a ligand-independent manner (Sweitzer et al., 1995), but not in untreated cells (Figs. 4D,E). Stat92E contains thirteen tyrosine residues, including Y^{711}, and presumably it is these other tyrosine residues that are phosphorylated after treatment with pervanadate (Hou et al., 1996; Yan et al., 1996).

Stat92E$^{\Delta N\Delta C}$ is a constitutive transcriptional co-activator and has dominant-active behavior *in vivo*

Strikingly, in the presence of Hop-Myc-His, Stat92E lacking both the N and C termini (Stat92E$^{\Delta N\Delta C}$) induced luciferase activity significantly more robustly than Stat92E^{FL} or than the single N- and C-terminal truncations, demonstrating that it has increased transcriptional activation capablities (Fig. 4A, Lane 7). Furthermore, Stat92E$^{\Delta N\Delta C}$ alone induced high levels of *socs1-luc* in the absence of Hop-Myc-His (Fig. 4A,B, Lanes 7). These data strongly suggest that the Stat92E$^{\Delta N\Delta C}$ protein is constitutively active. Importantly, ectopic expression of Stat92E$^{\Delta N\Delta C}$ with *ey-Gal4* resulted in moderate overgrowth of eye tissue (Fig. 5C). Despite low penetrance of this phenotype (~5%), the Stat92E$^{\Delta N\Delta C}$-induced

overgrowth is significant because this gain-of-function phenotype is never observed with ectopic expression of other *Stat92E* transgenes (Fig. 5A,B and Fig. S1).

To determine whether Stat92E$^{\Delta N\Delta C}$ exhibits constitutive activity in other tissues, we examined its ability to induce melanotic tumors. Ectopic expression of *UAS-hop* in flip-out clones resulted in ligand-independent, autonomous activation of Stat92E and gave rise to melanotic tumors (Fig. 5D and (Ekas et al., 2006)). Similarly, ectopic expression of Stat92E$^{\Delta N\Delta C}$ in flip-out clones also caused tumors (Fig. 5E). Melanotic tumors were never seen in clones mis-expressing Stat92E^{FL} (data not shown). Ectopic expression of Stat92E$^{\Delta N\Delta C}$ or Hop also induced cell-autonomous expression of an *in vivo* Stat92E transcriptional reporter (Fig. 5H, data not shown and (Bach et al., 2007)). By contrast, mis-expression of Stat92E^{FL} did not activate this reporter (data not shown). We tested constitutive nuclear localization or constitutive tyrosine phosphorylation as possible mechanisms for the dominant active behavior of Stat92E$^{\Delta N\Delta C}$. Stat92E$^{\Delta N\Delta C}$ is cytoplasmic in S2 cells in the absence of stimulation and translocates to the nucleus after activation, ruling out the former model (Fig. 5F,G). Stat92E$^{\Delta N\Delta C}$ was not tyrosine phosphorylated in untreated cells (Fig. 4E, Lane 5) but became tyrosine phosphorylated in response to pervanadate (Fig. 4D, Lane 5). These data suggest that the latter model is also not correct. However, Stat92E$^{\Delta N\Delta C}$ could contain levels of phosphotyrosine higher than endogenous Stat92E but below the level of detection of the PY-20 antibody used in this experiment

We determined that Stat92E$^{\Delta N\Delta C}$ acts epistatically to *upd* because its mis-expression specifically in the eye rescued the small-eye phenotype of *outstretched* (*os*), a viable *upd* allele that has small eyes and outstretched wings (Lindsley and Zimm, 1992). *upd* is an X-linked genes, and *os/Y* males or *os/os* females manifest these eye and wing phenotypes. We used *ey-Gal4* (Hauck et al., 1999) to drive expression of Stat92E$^{\Delta N\Delta C}$ in *os/Y* males and compared the size of the eye in *os/Y; Stat92E$^{\Delta N\Delta C}$/CyO* and *os/Y; Stat92E$^{\Delta N\Delta C}$/ey-Gal4* males (n=80 eyes for both genotypes). We found that *os/Y; Stat92E$^{\Delta N\Delta C}$/CyO* flies had adult eyes that were identical in size to *os/Y* males, indicating that the presence of the transgene alone does not generate a phenotype (Fig. 5I and data not shown). In contrast, *os/Y; Stat92E$^{\Delta N\Delta C}$/ey-Gal4* males had eyes that were nearly identical to those in wild type *+/Y* males and were significantly larger than those in *os/Y; Stat92E$^{\Delta N\Delta C}$/CyO* males, an observation that is statistically significant ($p<10^{-34}$, Student's T-test) (Fig. 5J,K). Notably, *ey>Stat92E$^{\Delta N\Delta C}$* did not rescue the outstretched wing phenotype of *os/Y* flies.

The dominant-active properties of Stat92E$^{\Delta N\Delta C}$ require Y^{711}

Tyrosine phosphorylation on conserved C-terminal tyrosine residues is required for the function of mammalian STATs and for the constitutive activity of Cys mutants STAT3-C and STAT1-C (Li and Shaw, 2006; Liddle et al., 2006). To examine whether this was also the case for Stat92E$^{\Delta N\Delta C}$, we generated a *Stat92E$^{\Delta N\Delta C}$* transgene that has a Tyr^{711} to Phe substitution (*Stat92E$^{\Delta N\Delta CY711F}$*). We found that either in the presence or in the absence of Hop, Stat92E$^{\Delta N\Delta CY711F}$ could not activate *socs1-luc* above background levels (Fig. 4C, Lanes 7,8). This is similar to the transcriptional co-activation abilities of a Stat92E that only contains a substitution of Tyr^{711} to Phe (Fig. 4A,B, Lanes 8). Therefore, the dominant-active abilities of Stat92E$^{\Delta N\Delta C}$ require phosphorylation of Tyr^{711} and by inference the formation of a phosphorylated, activated dimer.

Stat92E$^{\Delta N\Delta C}$ forms dimers with endogenous Stat92E following activation

To address whether the dominant-active behavior of Stat92E$^{\Delta N\Delta C}$ resulted from dimer formation with a functional Stat92E, we determined whether of Stat92E$^{\Delta N\Delta C}$ caused melanotic tumors in the absence of endogenous Stat92E. We generated positively-marked *Stat92E^{85C9}* clones that over-expressed Stat92E$^{\Delta N\Delta C}$ (see Materials and Methods). We were

unable to find any melanotic tumors despite the examination of hundreds of larvae harboring these clones (data not shown). These data indicate that Stat92E$^{\Delta N\Delta C}$ causes tumors and overgrowths only in tissues that contain a functional Stat92E protein. This conclusion is supported by the observations that Stat92E$^{\Delta N\Delta C}$ never caused over-growths in *Stat92E^{85C9} M^{+}* or *Stat92E^{397} M^{+}* mutant eye discs.

To address if there is a physical interaction between endogenous Stat92E and Stat92E$^{\Delta N\Delta C}$, we performed co-immunoprecipitation experiments in S2 cells. We found that in the absence of pervandate stimulation, endogenous Stat92E did not co-immunoprecipitate with either Stat92E^{FL} or Stat92E$^{\Delta N\Delta C}$ (Fig. 5L, Lanes 1,3,5,7). In contrast, after pervandate stimulation, endogenous Stat92E was detected in immuno-precipitates of both Stat92E^{FL} and Stat92E$^{\Delta N\Delta C}$ (Fig. 5L, Lanes 2,4,6,8). Taken together, these data indicate that endogenous Stat92E:Stat92E$^{\Delta N\Delta C}$ dimers are required for dominant-active behavior of Stat92E$^{\Delta N\Delta C}$.

Arg^{442} is required for Stat92E-induced transcriptional activation

The *Stat92E^{85C9}* allele results from a substitution of Pro for Arg at residue 442 (Fig. 1B) (Silver and Montell, 2001). This Arg residue is conserved in the *C. elegans* STAT, STA-1, and in mammalian STATs 2, 3, 5, and 6 (Fig. 7C and (Wang and Levy, 2006b;Yan et al., 1996)). To determine the functional importance of Arg at position 442 in Stat92E, we generated these constructs: *Stat92E^{R442P}*, which mimics the *85C9* mutation; *Stat92E^{R442K}*, which contains a conservative substitution of Arg^{442} to Lys; and *Stat92E^{R442A}*, which contains a non-conservative substitution of Arg^{442} to Ala. We found that Stat92E^{R442P} cannot rescue the *Stat92E* small-eye phenotype, shift the *85C9* lethal phase or activate transcription (Fig. 3J,M and Fig. 4A, B, Lanes 9), which is consistent with *Stat92E^{85C9}* being a strong hypomorph. We reasoned that if a positive charge were required at position 442, then Stat92E^{R442K} should be functional, while Stat92E^{R442A} should not. However, we found that neither of these Stat92E variants could rescue the *Stat92E* small-eye phenotype, shift the lethal phase or induces *socs1-luc* transcription (Fig. 3K,L,M;Fig. 4A, B, Lanes 10 and 11). Moreover, all of three Arg mutants had dominant-negative effects in a *Stat92E* hypomorphic background. The embryonic lethality of *85C9* zygotic homozygotes rose to more than 70% with the expression of these constructs, and the R^{442P}, R^{442K} and R^{442A} (as well as the Y^{711F}) crosses had to be set up for one year to collect 20 adult females for quantification of area of the eye (Figs. 3S and Fig. S1). We ruled out the possibility that the inactivity of the R442 mutants was due to aberrant expression (Fig. 4D,E, Lanes 7-9 and Fig. S2H-J). We also ruled out the possibility that R442 was required for nuclear translocation. Stat92E^{R442P} was cytosolic in the absence of stimulation, and translocated to the nucleus upon treatment with pervanadate, similar to endogenous Stat92E and Stat92E^{FL} (Fig. 6A-D,G,H). By contrast, Stat92E^{Y711F} remained cytoplasmic in both the presence and absence of stimulation, as has been observed for mammalian STATs (Fig. 6E,F and (Levy and Darnell, 2002)). Lastly, the R442 mutant proteins behaved like Stat92E^{FL} with regards to tyrosine phosphorylation: they contained undetectable levels of phospho-tyrosine in the absence of stimulation and high levels following pervanadate treatment (Fig. 4D,E, Lanes 7-9). We conclude that Arg^{442} is not required for Stat92E activation or for nuclear translocation but that it is indispensible for transcriptional co-activation by Stat92E.

Arg^{442} may directly contact the minor groove of the DNA helix

We reasoned that Arg^{442} may be important for maintaining a STAT-DNA interface. To test this hypothesis by observing where Arg^{442} is located on the 3D structure of Stat92E relative to bound DNA, we generated a homology model of Stat92E based on the crystallographic structure of a phosphorylated STAT1 dimer bound to DNA (Chen et al., 1998). This model revealed that Arg^{442} likely contacts DNA directly, presumably by accessing the minor

groove of the DNA helix (Fig. 7B). The model comfortably positions the Arg^{442} side chain with 484 A^2 surface area of contact with the DNA bases in the minor groove. Contact with the major groove or with other Stat92E binding partners is unlikely from this location as long as DNA is bound to Stat92E, since the loop on which Arg^{442} sits is nestled deeply in the minor groove and should not extend out of the minor groove even if it takes on a different conformation than that seen in the model. Interestingly, the location of Arg^{442} and the observation that Lys is not functional at this position in Stat92E suggest that only protein side chain:DNA interactions which depend exclusively on the Arg guanidinium group are operative here for Stat92E. The list of canonical candidate interactions of this type have been previously published (Luscombe et al., 2001), and only one is possible with the sequence of bases recognized by Stat92E, namely a complex, stacked base minor groove interaction with a cytosine and thymine. This complex would be lost with the $Stat92E^{R422}$ mutation to Pro, which eliminates the side-chain guanidinium group. Thus, our model and the observed data suggests that Arg^{442} interacts with the T and C of the TTCnnnGAA that is present in the optimal binding sites of nearly all STAT proteins, including Stat92E and STA-1 (Fig. 7D and (Decker et al., 1997)). These data suggest that Arg^{442} contributes to Stat92E's ability to recognize its target DNA binding site.

Discussion

In this study we use *in vivo* and *in vitro* assays to perform a structure-function analysis of Stat92E. We find that neither the N- terminus (residues 1-133) nor the C-terminus (residues 725-761) is required for Stat92E function *in vivo* and *in vitro*. However, when both N- and C-termini are removed, the resulting protein $Stat92E^{\Delta N\Delta C}$ has dominant-active properties, including oncogenesis. Furthermore, we demonstrate that $Stat92E^{\Delta N\Delta C}$ with a Tyr to Phe substitution at residue 711 ($Stat92E^{\Delta N\Delta CY711F}$) is non-functional. We also showed that both $Stat92E^{Y711F}$ and $Stat92E^{R442P}$ are non-functional and manifested dominant-negative activities *in vivo*. The lack of function of the $Stat92E^{Y711F}$ variant is likely due to an inability to form an activated dimer, as has been previously reported (Yan et al., 1996). Our data suggest that $Stat92E^{R442P}$ cannot function because it does not maintain normal interactions between activated Stat92E dimers and cognate DNA.

Our study is important for several reasons, perhaps foremost of which is that we are the first group to identify a dominant-active Stat92E. The simultaneous removal of the N-terminal 133 and the C-terminal 36 amino acids results in a truncated protein that has constitutive activity, which causes melanotic tumors when mis-expressed in wild type larvae and transactivates a Stat92E reporter genes *in vitro* and *in vivo* in the absence of stimulation. We show that the activity of $Stat92E^{\Delta N\Delta C}$ is dependent on the presence of Y^{711}, as is that of $Stat92E^{FL}$. These data suggest that $Stat92E^{\Delta N\Delta C}$ is activated in a manner similar to full length Stat92E (i.e., by reciprocal interactions between SH2 domains and phosphorylated Y^{711} residues on adjacent Stat92E protein). Consistent with this, we show that $Stat92E^{\Delta N\Delta C}$ forms a dimer with endogenous Stat92E (i.e., a Stat92E: $Stat92E^{\Delta N\Delta C}$ dimer) after pervanadate stimulation. Therefore, $Stat92E^{\Delta N\Delta C}$ appears to behave like wild type Stat92E that has lost a negative regulatory component. One possibility is that removal of the N- and C-termini prolongs the interaction between the Stat92E: $Stat92E^{\Delta N\Delta C}$ dimer and DNA, leading to increased gene activation. Another is that Stat92E:$Stat92E^{\Delta N\Delta C}$ dimers cannot be efficiently dephosphorylated and/or return to a parallel dimer conformation, which may be required for normal export of Stat92E dimers to the cytoplasm (Chen et al., 2003). Constitutive activity is not observed by the removal of either the N or C-terminus domain individually, and therefore, deletion of the both domains must contribute to this activity. The constitutive activity of $Stat92E^{\Delta N\Delta C}$ *in vitro* is significantly robust that it could be used for RNAi screens to identify enhancers and suppressors of Stat92E activity, which may have conserved functions in restricting tumorigenesis in mammals. In addition, the high rate of

melanotic tumor formation observed in clones mis-expressing Stat92E$^{\Delta N\Delta C}$ will make this mutation an extremely useful *in vivo* reagent as well.

One unresolved issue is how the constitutive activity of Stat92E$^{\Delta N\Delta C}$ is initiated in the first place. The model described above predicts that in the absence of stimulation (1) Stat92E:Stat92E$^{\Delta N\Delta C}$ dimers should be detected, if only at very low levels, and/or (2) Stat92E$^{\Delta N\Delta C}$ should be tyrosine phosphorylated, again if only at very low levels. Unexpectedly neither result is observed. To rectify these results, we invoke a model in which a few activated STAT dimers (in this case Stat92E: Stat92E$^{\Delta N\Delta C}$ dimers) are constantly generated within a cell, and their activity is quenched by tyrosine phosphatases (Fig. 7A). Although we have not been able to detect these dimers, we know that this is a plausible model because treatment of a cell with vanadate, a pan-phosphatase inhibitor, activates STATs in a ligand-independent manner *in vivo* and *in vitro*, presumably by inhibiting the enzymes that keep their low level of activation in check (Duff et al., 1997;Sweitzer et al., 1995;Tourkine et al., 1995). We hypothesize that Stat92E:Stat92E$^{\Delta N\Delta C}$ dimers may better evade the actions of tyrosine phosphatases, resulting in a steady state of increased STAT signaling in a cell and ultimately leading sustained increased expression of STAT targets and, in certain cell types like the blood, oncogenesis.

As mentioned above, we also discovered that Stat92E lacking either the N- or the C-terminus functioned similarly to Stat92E^{FL}. They rescued the eye/antennal/head phenotypes, as well as the hatching rate, and they shifted the lethality in either *85C9/85C9* or *397/397* zygotic mutants. The fact that a transgene encoding a Stat92E lacking the last 36 amino acids could rescue the phenotypes associated with homozygosity for the *397* allele, which is predicted to encode a protein lacking all amino acids after Trp594, suggest that the transactivation domain of Stat92E does not residue at the C-terminus, since a Stat92E$^{\Delta C}$: Stat92E^{397} dimer would lack any residue after 724. Alternatively, there could be more than one transactivation domain in Stat92E, one at the C-terminus and the other located elsewhere in the protein. The proteins encoded by the *Stat92E^{85C9}* and *Stat92E^{397}* alleles are predicted to have N-terminal domains (this work and (Silver and Montell, 2001)). Previous work has shown that two N-termini are required for the formation of non-phosphorylated dimers, which are the preferred substrated of receptor/JAK complexes and are required for cytokine-dependent activation of STAT4 (Chang et al., 2003; Chen et al., 2003; Murphy et al., 2000; Ota et al., 2004; Shuai et al., 1996). As such, the single N-terminus present in any potential dimers between Stat92E$^{\Delta N}$ and Stat92E^{85C9} or between Stat92E$^{\Delta N}$ and Stat92E^{397} is unlikely to support dimer formation/activation in *Stat92E^{85C9}* and *Stat92E^{397}* homozygous mutant cells, respectively.

Our results showing that Stat92E$^{\Delta N}$ can function like Stat92E^{FL} differ from those reported by two other groups (Henriksen et al., 2002; Karsten et al., 2006). The former authors reported that a Stat92E lacking the first 133 residues was generated by transcription of an alternative promoter in response to pathway activation and acted as dominant negative *in vivo*. Mis-expression of their Stat92E$^{\Delta N}$ construct in wild type embryos led to the same phenotype as complete loss of *Stat92E:* the loss of expression of *even-skipped* stripes 3, 5 and 7 (Henriksen et al., 2002; Hou et al., 1996). The latter group reported that mis-expression of a Stat92E$^{\Delta N}$ protein tagged at the C-terminal by GFP (Stat92E$^{\Delta N}$–GFP) in the embryo abrogated expression of *trachealess*, which is also lost in embryos null for *dome* gene (Brown et al., 2001; Chen et al., 2002; Karsten et al., 2006). The reason for the discrepacy between our and their results is not clear at present.

Our study is also noteworthy in that it is the first analysis of Stat92E structure-function variants that employs *in vivo* rescue assays in a *Stat92E* homozygous mutant background. We previously reported that 90% of animals carrying large patches of *Stat92E* homozygous

mutant tissue in the eye-antennal disc fail to hatch but that these phenotypes were rescued when these animals expressed a full-length version of Stat92E in the eye-antennal disc (this study and (Ekas et al., 2006)). We now show that mis-expression of $Stat92E^{FL}$ in *85C9/85C9* zygotic mutants significantly shifted the lethal phase, from embryonic/first larval instar to third larval instar/early pupa. Currently we do not understand why the *UASp-3HA-*$Stat92E^{FL}$ transgene did not rescue to *85C9/85C9* homozygotes to adulthood, but one possibility is low expression. Transgenes driven by *UASp*, which are designed for expression in the germ-line (Rorth, 1996), are expressed at significantly lower levels of than those driven by *UAST*, which are expressed in the soma (Brand and Perrimon, 1993), and the levels of Stat92E required to rescue to *85C9* or *397* zygotic mutants to adulthood simply might not have been achieved.

We are the first to demonstrate that Tyr^{711} is required for Stat92E function *in vivo*, which is consistent with *in vitro* data that a substitution of Tyr^{711} to Phe abolished the ability of Stat92E to bind DNA (Karsten et al., 2006; Yan et al., 1996). However, we do not observe a reduction in eye size when we over-express this Stat92E construct in a wild type fly eye. We believe that this is due to our inability to over-express this construct at high enough levels to inhibit the function of endogenous Stat92E. Finally, we have also shown that an Arg residue is specifically required at position 442 for Stat92E function. Our homology model of Stat92E suggests that Arg^{442} is involved in DNA binding and may be a recognition element for the binucleotide TTCnnnGAA in the Stat92E binding site, suggesting that this interaction may be important for Stat92E recognition of its DNA target site. The Arg^{442} of Stat92E is conserved in the *C. elegans* STAT, STA-1, and in all mammalian STAT2,3,5a,5b and 6. Therefore, it will be interesting in the future to determine if this residue is also required for the function of STAT proteins in which this Arg residue is conserved.

Supplementary Material

Refer to Web version on PubMed Central for supplementary material.

Acknowledgments

We are indebted to Kent Nybakken for providing the *C5HA3* vector prior to publication (Nybakken et al., 2005), to Uwe Vinkemeier for several key reagents, to Steve Hubbard for help with the Arg^{442} mutations and to Tempei Ikegame for making *socs1-luc*. We thank Ram Dasgupta, Jessica Treisman, Norbert Perrimon and the Bloomington Stock Center for fly stocks and reagents. Several mAbs used in this study were obtained from the DSHB, Department of Biological Sciences, Iowa City, IA 52242. We thank David Levy, Mark Chong, Lawrence Gardner and Yaming Wang and Ines Carrera, and members of the Bach and Dasgupta labs for helpful comments and guidance.

This project was support in part by a Basil O'Connor Starter Scholar Research Award (Grant No.: 5-FY06) from the March of Dimes Foundation to E.A.B; by an NIH institutional training grant (T32 GM066704-03) to L.A.E.; by a Research Scholar Grant (RSG-DDD-115829) from the American Cancer Society to E.A.B.; and a National Institutes of Health grant from NIGMS (1R01GM085075) to E.A.B.

References

Agaisse H, Petersen UM, Boutros M, Mathey-Prevot B, Perrimon N. Signaling Role of Hemocytes in Drosophila JAK/STAT-Dependent Response to Septic Injury. Dev Cell. 2003; 5:441–450. [PubMed: 12967563]

Arbouzova NI, Zeidler MP. JAK/STAT signalling in Drosophila: insights into conserved regulatory and cellular functions. Development. 2006; 133:2605–2616. [PubMed: 16794031]

Ayala-Camargo A, Ekas LA, Flaherty MS, Baeg GH, Bach EA. The JAK/STAT pathway regulates proximo-distal patterning in Drosophila. Dev Dyn. 2007; 236:2721–2730. [PubMed: 17626283]

Bach EA, Ekas LA, Ayala-Camargo A, Flaherty MS, Lee H, Perrimon N, Baeg GH. GFP reporters detect the activation of the Drosophila JAK/STAT pathway in vivo. Gene Expr Patterns. 2007; 7:323–331. [PubMed: 17008134]

Bach EA, Tanner JW, Marsters S, Ashkenazi A, Aguet M, Shaw AS, Schreiber RD. Ligand-induced assembly and activation of the gamma interferon receptor in intact cells. Mol Cell Biol. 1996; 16:3214–3221. [PubMed: 8649432]

Bach EA, Vincent S, Zeidler MP, Perrimon N. A sensitized genetic screen to identify novel regulators and components of the Drosophila janus kinase/signal transducer and activator of transcription pathway. Genetics. 2003; 165:1149–1166. [PubMed: 14668372]

Baeg GH, Zhou R, Perrimon N. Genome-wide RNAi analysis of JAK/STAT signaling components in *Drosophila*. Genes Dev. 2005; 19:1861–1870. [PubMed: 16055650]

Baxter EJ, Scott LM, Campbell PJ, East C, Fourouclas N, Swanton S, Vassiliou GS, Bench AJ, Boyd EM, Curtin N, Scott MA, Erber WN, Green AR. Acquired mutation of the tyrosine kinase JAK2 in human myeloproliferative disorders. Lancet. 2005; 365:1054–1061. [PubMed: 15781101]

Becker S, Groner B, Muller CW. Three-dimensional structure of the Stat3beta homodimer bound to DNA. Nature. 1998; 394:145–151. [PubMed: 9671298]

Binari R, Perrimon N. Stripe-specific regulation of pair-rule genes by hopscotch, a putative Jak family tyrosine kinase in Drosophila. Genes Dev. 1994; 8:300–312. [PubMed: 8314084]

Blaskovich MA, Sun J, Cantor A, Turkson J, Jove R, Sebti SM. Discovery of JSI-124 (cucurbitacin I), a selective Janus kinase/signal transducer and activator of transcription 3 signaling pathway inhibitor with potent antitumor activity against human and murine cancer cells in mice. Cancer Res. 2003; 63:1270–1279. [PubMed: 12649187]

Brand AH, Perrimon N. Targeted gene expression as a means of altering cell fates and generating dominant phenotypes. Development. 1993; 118:401–415. [PubMed: 8223268]

Braunstein J, Brutsaert S, Olson R, Schindler C. STATs dimerize in the absence of phosphorylation. J Biol Chem. 2003; 278:34133–34140. [PubMed: 12832402]

Bromberg JF, Wrzeszczynska MH, Devgan G, Zhao Y, Pestell RG, Albanese C, Darnell JE Jr. Stat3 as an oncogene. Cell. 1999; 98:295–303. [PubMed: 10458605]

Brown S, Hu N, Hombria JC. Identification of the first invertebrate interleukin JAK/STAT receptor, the Drosophila gene domeless. Curr Biol. 2001; 11:1700–1705. [PubMed: 11696329]

Brown S, Hu N, Hombria JC. Novel level of signalling control in the JAK/STAT pathway revealed by in situ visualisation of protein-protein interaction during Drosophila development. Development. 2003; 130:3077–3084. [PubMed: 12783781]

Callus BA, Mathey-Prevot B. SOCS36E, a novel Drosophila SOCS protein, suppresses JAK/STAT and EGF-R signalling in the imaginal wing disc. Oncogene. 2002; 21:4812–4821. [PubMed: 12101419]

Cardozo T, Totrov M, Abagyan R. Homology modeling by the ICM method. Proteins. 1995; 23:403–414. [PubMed: 8710833]

Chang HC, Zhang S, Oldham I, Naeger L, Hoey T, Kaplan MH. STAT4 requires the N-terminal domain for efficient phosphorylation. J Biol Chem. 2003; 278:32471–32477. [PubMed: 12805384]

Chao JL, Tsai YC, Chiu SJ, Sun YH. Localized Notch signal acts through eyg and upd to promote global growth in Drosophila eye. Development. 2004; 131:3839–3847. [PubMed: 15253935]

Chen HW, Chen X, Oh SW, Marinissen MJ, Gutkind JS, Hou SX. mom identifies a receptor for the Drosophila JAK/STAT signal transduction pathway and encodes a protein distantly related to the mammalian cytokine receptor family. Genes Dev. 2002; 16:388–398. [PubMed: 11825879]

Chen X, Bhandari R, Vinkemeier U, Van Den Akker F, Darnell JE Jr, Kuriyan J. A reinterpretation of the dimerization interface of the N-terminal domains of STATs. Protein Sci. 2003; 12:361–365. [PubMed: 12538899]

Chen X, Vinkemeier U, Zhao Y, Jeruzalmi D, Darnell JE Jr, Kuriyan J. Crystal structure of a tyrosine phosphorylated STAT-1 dimer bound to DNA. Cell. 1998; 93:827–839. [PubMed: 9630226]

Chiarle R, Simmons WJ, Cai H, Dhall G, Zamo A, Raz R, Karras JG, Levy DE, Inghirami G. Stat3 is required for ALK-mediated lymphomagenesis and provides a possible therapeutic target. Nat Med. 2005; 11:623–629. [PubMed: 15895073]

Darnell JE. Validating Stat3 in cancer therapy. Nat Med. 2005; 11:595–596. [PubMed: 15937466]

DasGupta R, Kaykas A, Moon RT, Perrimon N. Functional genomic analysis of the Wnt-wingless signaling pathway. Science. 2005; 308:826–833. [PubMed: 15817814]

Decker T, Kovarik P, Meinke A. GAS elements: a few nucleotides with a major impact on cytokine-induced gene expression. J Interferon Cytokine Res. 1997; 17:121–134. [PubMed: 9085936]

Dominguez M, Casares F. Organ specification-growth control connection: new in-sights from the Drosophila eye-antennal disc. Dev Dyn. 2005; 232:673–684. [PubMed: 15704149]

Duff JL, Quinlan KL, Paxton LL, Naik SM, Caughman SW. Pervanadate mimics IFNgamma-mediated induction of ICAM-1 expression via activation of STAT proteins. J Invest Dermatol. 1997; 108:295–301. [PubMed: 9036928]

Ekas LA, Baeg GH, Flaherty MS, Ayala-Camargo A, Bach EA. JAK/STAT signaling promotes regional specification by negatively regulating wingless expression in Drosophila. Development. 2006; 133:4721–4729. [PubMed: 17079268]

Flaherty MS, Salis P, Evans CJ, Ekas LA, Marouf A, Zavadil J, Banerjee U, Bach EA. *chinmo* is a functional effector of the JAK/STAT pathway that regulates eye development, tumor formation and stem cell self-renewal in *Drosophila*. Developmental Cell. in press. 10.1016/j.devcel.2010.02.006

Flaherty MS, Zavadil J, Ekas LA, Bach EA. Genome-wide expression profiling in the Drosophila eye reveals unexpected repression of notch signaling by the JAK/STAT pathway. Dev Dyn. 2009; 238:2235–2253. [PubMed: 19504457]

Gilbert MM, Weaver BK, Gergen JP, Reich NC. A novel functional activator of the Drosophila JAK/STAT pathway, unpaired2, is revealed by an in vivo reporter of pathway activation. Mech Dev. 2005; 122:939–948. [PubMed: 15925495]

Hanratty WP, Dearolf CR. The Drosophila Tumorous-lethal hematopoietic oncogene is a dominant mutation in the hopscotch locus. Mol Gen Genet. 1993; 238:33–37. [PubMed: 8479437]

Harrison DA, Binari R, Nahreini TS, Gilman M, Perrimon N. Activation of a Drosophila Janus kinase (JAK) causes hematopoietic neoplasia and developmental defects. Embo J. 1995; 14:2857–2865. [PubMed: 7796812]

Harrison DA, McCoon PE, Binari R, Gilman M, Perrimon N. Drosophila unpaired encodes a secreted protein that activates the JAK signaling pathway. Genes Dev. 1998; 12:3252–3263. [PubMed: 9784499]

Hauck B, Gehring WJ, Walldorf U. Functional analysis of an eye specific enhancer of the eyeless gene in Drosophila. Proc Natl Acad Sci U S A. 1999; 96:564–569. [PubMed: 9892673]

Henriksen MA, Betz A, Fuccillo MV, Darnell JE Jr. Negative regulation of STAT92E by an N-terminally truncated STAT protein derived from an alternative promoter site. Genes Dev. 2002; 16:2379–2389. [PubMed: 12231627]

Herz HM, Chen Z, Scherr H, Lackey M, Bolduc C, Bergmann A. vps25 mosaics display non-autonomous cell survival and overgrowth, and autonomous apoptosis. Development. 2006; 133:1871–1880. [PubMed: 16611691]

Hombria JC, Brown S, Hader S, Zeidler MP. Characterisation of Upd2, a Drosophila JAK/STAT pathway ligand. Dev Biol. 2005; 288:420–433. [PubMed: 16277982]

Horvath CM. STAT proteins and transcriptional responses to extracellular signals. Trends Biochem Sci. 2000; 25:496–502. [PubMed: 11050435]

Hou XS, Melnick MB, Perrimon N. Marelle acts downstream of the Drosophila HOP/JAK kinase and encodes a protein similar to the mammalian STATs. Cell. 1996; 84:411–419. [PubMed: 8608595]

Issigonis M, Tulina N, de Cuevas M, Brawley C, Sandler L, Matunis E. JAK-STAT signal inhibition regulates competition in the Drosophila testis stem cell niche. Science. 2009; 326:153–156. [PubMed: 19797664]

Ito K, Awano W, Suzuki K, Hiromi Y, Yamamoto D. The Drosophila mushroom body is a quadruple structure of clonal units each of which contains a virtually identical set of neurones and glial cells. Development. 1997; 124:761–771. [PubMed: 9043058]

James C, Ugo V, Le Couedic JP, Staerk J, Delhommeau F, Lacout C, Garcon L, Raslova H, Berger R, Bennaceur-Griscelli A, Villeval JL, Constantinescu SN, Casadevall N, Vainchenker W. A unique clonal JAK2 mutation leading to constitutive signalling causes polycythaemia vera. Nature. 2005; 434:1144–1148. [PubMed: 15793561]

Janody F, Lee JD, Jahren N, Hazelett DJ, Benlali A, Miura GI, Draskovic I, Treisman JE. A mosaic genetic screen reveals distinct roles for trithorax and polycomb group genes in Drosophila eye development. Genetics. 2004; 166:187–200. [PubMed: 15020417]

Jones AV, Chase A, Silver RT, Oscier D, Zoi K, Wang YL, Cario H, Pahl HL, Collins A, Reiter A, Grand F, Cross NC. JAK2 haplotype is a major risk factor for the development of myeloproliferative neoplasms. Nat Genet. 2009; 41:446–449. [PubMed: 19287382]

Juni N, Awasaki T, Yoshida K, Hori SH. The Om (1E) mutation in Drosophila ananassae causes compound eye overgrowth due to tom retrotransposon-driven overexpression of a novel gene. Genetics. 1996; 143:1257–1270. [PubMed: 8807298]

Karsten P, Hader S, Zeidler MP. Cloning and expression of Drosophila SOCS36E and its potential regulation by the JAK/STAT pathway. Mech Dev. 2002; 117:343–346. [PubMed: 12204282]

Karsten P, Plischke I, Perrimon N, Zeidler MP. Mutational analysis reveals separable DNA binding and trans-activation of Drosophila STAT92E. Cell Signal. 2006; 18:819–829. [PubMed: 16129580]

Kilpivaara O, Mukherjee S, Schram AM, Wadleigh M, Mullally A, Ebert BL, Bass A, Marubayashi S, Heguy A, Garcia-Manero G, Kantarjian H, Offit K, Stone RM, Gilliland DG, Klein RJ, Levine RL. A germline JAK2 SNP is associated with predisposition to the development of JAK2(V617F)-positive myeloproliferative neoplasms. Nat Genet. 2009; 41:455–459. [PubMed: 19287384]

Klueg KM, Alvarado D, Muskavitch MA, Duffy JB. Creation of a GAL4/UAS-coupled inducible gene expression system for use in Drosophila cultured cell lines. Genesis. 2002; 34:119–122. [PubMed: 12324964]

Kretzschmar AK, Dinger MC, Henze C, Brocke-Heidrich K, Horn F. Analysis of Stat3 (signal transducer and activator of transcription 3) dimerization by fluorescence resonance energy transfer in living cells. Biochem J. 2004; 377:289–297. [PubMed: 12974672]

Lacronique V, Boureux A, Valle VD, Poirel H, Quang CT, Mauchauffe M, Berthou C, Lessard M, Berger R, Ghysdael J, Bernard OA. A TEL-JAK2 fusion protein with constitutive kinase activity in human leukemia. Science. 1997; 278:1309–1312. [PubMed: 9360930]

Lambertsson A. The minute genes in Drosophila and their molecular functions. Adv Genet. 1998; 38:69–134. [PubMed: 9677706]

Lee T, Luo L. Mosaic analysis with a repressible cell marker for studies of gene function in neuronal morphogenesis. Neuron. 1999; 22:451–461. [PubMed: 10197526]

Levine RL, Wadleigh M, Cools J, Ebert BL, Wernig G, Huntly BJ, Boggon TJ, Wlodarska I, Clark JJ, Moore S, Adelsperger J, Koo S, Lee JC, Gabriel S, Mercher T, D'Andrea A, Frohling S, Dohner K, Marynen P, Vandenberghe P, Mesa RA, Tefferi A, Griffin JD, Eck MJ, Sellers WR, Meyerson M, Golub TR, Lee SJ, Gilliland DG. Activating mutation in the tyrosine kinase JAK2 in polycythemia vera, essential thrombocythemia, and myeloid metaplasia with myelofibrosis. Cancer Cell. 2005; 7:387–397. [PubMed: 15837627]

Levy DE, Darnell JE Jr. Stats: transcriptional control and biological impact. Nat Rev Mol Cell Biol. 2002; 3:651–662. [PubMed: 12209125]

Li L, Shaw PE. Elevated activity of STAT3C due to higher DNA binding affinity of phosphotyrosine dimer rather than covalent dimer formation. J Biol Chem. 2006; 281:33172–33181. [PubMed: 16956893]

Liddle FJ, Alvarez JV, Poli V, Frank DA. Tyrosine phosphorylation is required for functional activation of disulfide-containing constitutively active STAT mutants. Biochemistry. 2006; 45:5599–5605. [PubMed: 16634641]

Lindsley DL, Zimm GG. The Genome of Drosophila melanogaster. 1992

Luo H, Hanratty WP, Dearolf CR. An amino acid substitution in the Drosophila hopTum-l Jak kinase causes leukemia-like hematopoietic defects. Embo J. 1995; 14:1412–1420. [PubMed: 7729418]

Luscombe NM, Laskowski RA, Thornton JM. Amino acid-base interactions: a three-dimensional analysis of protein-DNA interactions at an atomic level. Nucleic Acids Res. 2001; 29:2860–2874. [PubMed: 11433033]

Mao X, Ren Z, Parker GN, Sondermann H, Pastorello MA, Wang W, McMurray JS, Demeler B, Darnell JE Jr, Chen X. Structural bases of unphosphorylated STAT1 association and receptor binding. Mol Cell. 2005; 17:761–771. [PubMed: 15780933]

Mertens C, Zhong M, Krishnaraj R, Zou W, Chen X, Darnell JE Jr. Dephosphorylation of phosphotyrosine on STAT1 dimers requires extensive spatial reorientation of the monomers facilitated by the N-terminal domain. Genes Dev. 2006; 20:3372–3381. [PubMed: 17182865]

Moberg KH, Schelble S, Burdick SK, Hariharan IK. Mutations in erupted, the Drosophila ortholog of mammalian tumor susceptibility gene 101, elicit non-cell-autonomous overgrowth. Dev Cell. 2005; 9:699–710. [PubMed: 16256744]

Morata G, Ripoll P. Minutes: mutants of drosophila autonomously affecting cell division rate. Dev Biol. 1975; 42:211–221. [PubMed: 1116643]

Mukherjee T, Hombria JC, Zeidler MP. Opposing roles for Drosophila JAK/STAT signalling during cellular proliferation. Oncogene. 2005; 24:2503–2511. [PubMed: 15735706]

Murphy TL, Geissal ED, Farrar JD, Murphy KM. Role of the Stat4 N domain in receptor proximal tyrosine phosphorylation. Mol Cell Biol. 2000; 20:7121–7131. [PubMed: 10982828]

Neculai D, Neculai AM, Verrier S, Straub K, Klumpp K, Pfitzner E, Becker S. Structure of the unphosphorylated STAT5a dimer. J Biol Chem. 2005; 280:40782–40787. [PubMed: 16192273]

Novak U, Ji H, Kanagasundaram V, Simpson R, Paradiso L. STAT3 forms stable homodimers in the presence of divalent cations prior to activation. Biochem Biophys Res Commun. 1998; 247:558–563. [PubMed: 9647732]

Nybakken K, Vokes SA, Lin TY, McMahon AP, Perrimon N. A genome-wide RNA interference screen in Drosophila melanogaster cells for new components of the Hh signaling pathway. Nat Genet. 2005; 37:1323–1332. [PubMed: 16311596]

Olcaydu D, Harutyunyan A, Jager R, Berg T, Gisslinger B, Pabinger I, Gisslinger H, Kralovics R. A common JAK2 haplotype confers susceptibility to myeloproliferative neoplasms. Nat Genet. 2009; 41:450–454. [PubMed: 19287385]

Ota N, Brett TJ, Murphy TL, Fremont DH, Murphy KM. N-domain-dependent nonphosphorylated STAT4 dimers required for cytokine-driven activation. Nat Immunol. 2004; 5:208–215. [PubMed: 14704793]

Rawlings JS, Rennebeck G, Harrison SM, Xi R, Harrison DA. Two Drosophila suppressors of cytokine signaling (SOCS) differentially regulate JAK and EGFR pathway activities. BMC Cell Biol. 2004; 5:38. [PubMed: 15488148]

Reich NC, Liu L. Tracking STAT nuclear traffic. Nat Rev Immunol. 2006; 6:602–612. [PubMed: 16868551]

Reynolds-Kenneally J, Mlodzik M. Notch signaling controls proliferation through cell-autonomous and non-autonomous mechanisms in the Drosophila eye. Dev Biol. 2005; 285:38–48. [PubMed: 16039641]

Rorth P. A modular misexpression screen in Drosophila detecting tissue-specific phenotypes. Proc Natl Acad Sci U S A. 1996; 93:12418–12422. [PubMed: 8901596]

Schroder M, Kroeger KM, Volk HD, Eidne KA, Grutz G. Preassociation of nonactivated STAT3 molecules demonstrated in living cells using bioluminescence resonance energy transfer: a new model of STAT activation? J Leukoc Biol. 2004; 75:792–797. [PubMed: 14742639]

Sefton L, Timmer JR, Zhang Y, Beranger F, Cline TW. An extracellular activator of the Drosophila JAK/STAT pathway is a sex-determination signal element. Nature. 2000; 405:970–973. [PubMed: 10879541]

Shuai K, Liao J, Song MM. Enhancement of antiproliferative activity of gamma interferon by the specific inhibition of tyrosine dephosphorylation of Stat1. Mol Cell Biol. 1996; 16:4932–4941. [PubMed: 8756652]

Silver DL, Montell DJ. Paracrine signaling through the JAK/STAT pathway activates invasive behavior of ovarian epithelial cells in Drosophila. Cell. 2001; 107:831–841. [PubMed: 11779460]

Song H, Wang R, Wang S, Lin J. A low-molecular-weight compound discovered through virtual database screening inhibits Stat3 function in breast cancer cells. Proc Natl Acad Sci U S A. 2005; 102:4700–4705. [PubMed: 15781862]

Spradling AC, Stern D, Beaton A, Rhem EJ, Laverty T, Mozden N, Misra S, Rubin GM. The Berkeley Drosophila Genome Project gene disruption project: Single P-element insertions mutating 25% of vital Drosophila genes. Genetics. 1999; 153:135–177. [PubMed: 10471706]

Stancato LF, David M, Carter-Su C, Larner AC, Pratt WB. Preassociation of STAT1 with STAT2 and STAT3 in separate signalling complexes prior to cytokine stimulation. J Biol Chem. 1996; 271:4134–4137. [PubMed: 8626752]

Stowers RS, Schwarz TL. A genetic method for generating Drosophila eyes composed exclusively of mitotic clones of a single genotype. Genetics. 1999; 152:1631–1639. [PubMed: 10430588]

Sun J, Blaskovich MA, Jove R, Livingston SK, Coppola D, Sebti SM. Cucurbitacin Q: a selective STAT3 activation inhibitor with potent antitumor activity. Oncogene. 2005; 24:3236–3245. [PubMed: 15735720]

Sweitzer SM, Calvo S, Kraus MH, Finbloom DS, Larner AC. Characterization of a Stat-like DNA binding activity in Drosophila melanogaster. J Biol Chem. 1995; 270:16510–16513. [PubMed: 7622453]

Thompson BJ, Mathieu J, Sung HH, Loeser E, Rorth P, Cohen SM. Tumor suppressor properties of the ESCRT-II complex component Vps25 in Drosophila. Dev Cell. 2005; 9:711–720. [PubMed: 16256745]

Tourkine N, Schindler C, Larose M, Houdebine LM. Activation of STAT factors by prolactin, interferon-gamma, growth hormones, and a tyrosine phosphatase inhibitor in rabbit primary mammary epithelial cells. J Biol Chem. 1995; 270:20952–20961. [PubMed: 7673119]

Tsai YC, Y JG, C PH, Posakony JW, Barolo S, Kim J, Henry Sun Y. Upd/Jak/STAT signaling represses wg transcription to allow initiation of morphogenetic furrow in Drosophila eye development. Dev Biol. 2007; 306:760–771. [PubMed: 17498684]

Tsai YC, Sun YH. Long-range effect of upd, a ligand for Jak/STAT pathway, on cell cycle in Drosophila eye development. Genesis. 2004; 39:141–153. [PubMed: 15170700]

Vaccari T, Bilder D. The Drosophila tumor suppressor vps25 prevents nonautonomous overproliferation by regulating notch trafficking. Dev Cell. 2005; 9:687–698. [PubMed: 16256743]

Vinkemeier U, Moarefi I, Darnell JE Jr, Kuriyan J. Structure of the amino-terminal protein interaction domain of STAT-4. Science. 1998; 279:1048–1052. [PubMed: 9461439]

Wang Y, Levy DE. C. elegans STAT cooperates with DAF-7/TGF-beta signaling to repress dauer formation. Curr Biol. 2006a; 16:89–94. [PubMed: 16401427]

Wang Y, Levy DE. C. elegans STAT: evolution of a regulatory switch. Faseb J. 2006b; 20:1641–1652. [PubMed: 16873887]

Xu T, Rubin GM. Analysis of genetic mosaics in developing and adult Drosophila tissues. Development. 1993; 117:1223–1237. [PubMed: 8404527]

Xu X, Sun YL, Hoey T. Cooperative DNA binding and sequence-selective recognition conferred by the STAT amino-terminal domain. Science. 1996; 273:794–797. [PubMed: 8670419]

Yan R, Small S, Desplan C, Dearolf CR, Darnell JE Jr. Identification of a Stat gene that functions in Drosophila development. Cell. 1996; 84:421–430. [PubMed: 8608596]

Yang E, Henriksen MA, Schaefer O, Zakharova N, Darnell JE Jr. Dissociation time from DNA determines transcriptional function in a STAT1 linker mutant. J Biol Chem. 2002; 277:13455–13462. [PubMed: 11834743]

Zeidler MP, Bach EA, Perrimon N. The roles of the Drosophila JAK/STAT pathway. Oncogene. 2000; 19:2598–2606. [PubMed: 10851058]

Zeidler MP, Perrimon N, Strutt DI. Polarity determination in the Drosophila eye: a novel role for unpaired and JAK/STAT signaling. Genes Dev. 1999; 13:1342–1353. [PubMed: 10346822]

Zeidler MP, Tan C, Bellaiche Y, Cherry S, Hader S, Gayko U, Perrimon N. Temperature-sensitive control of protein activity by conditionally splicing inteins. Nat Biotechnol. 2004; 22:871–876. [PubMed: 15184905]

Zhang X, Wrzeszczynska MH, Horvath CM, Darnell JE Jr. Interacting regions in Stat3 and c-Jun that participate in cooperative transcriptional activation. Mol Cell Biol. 1999; 19:7138–7146. [PubMed: 10490649]

Zhong M, Henriksen MA, Takeuchi K, Schaefer O, Liu B, ten Hoeve J, Ren Z, Mao X, Chen X, Shuai K, Darnell JE Jr. Implications of an antiparallel dimeric structure of nonphosphorylated STAT1 for the activation-inactivation cycle. Proc Natl Acad Sci U S A. 2005; 102:3966–3971. [PubMed: 15753310]

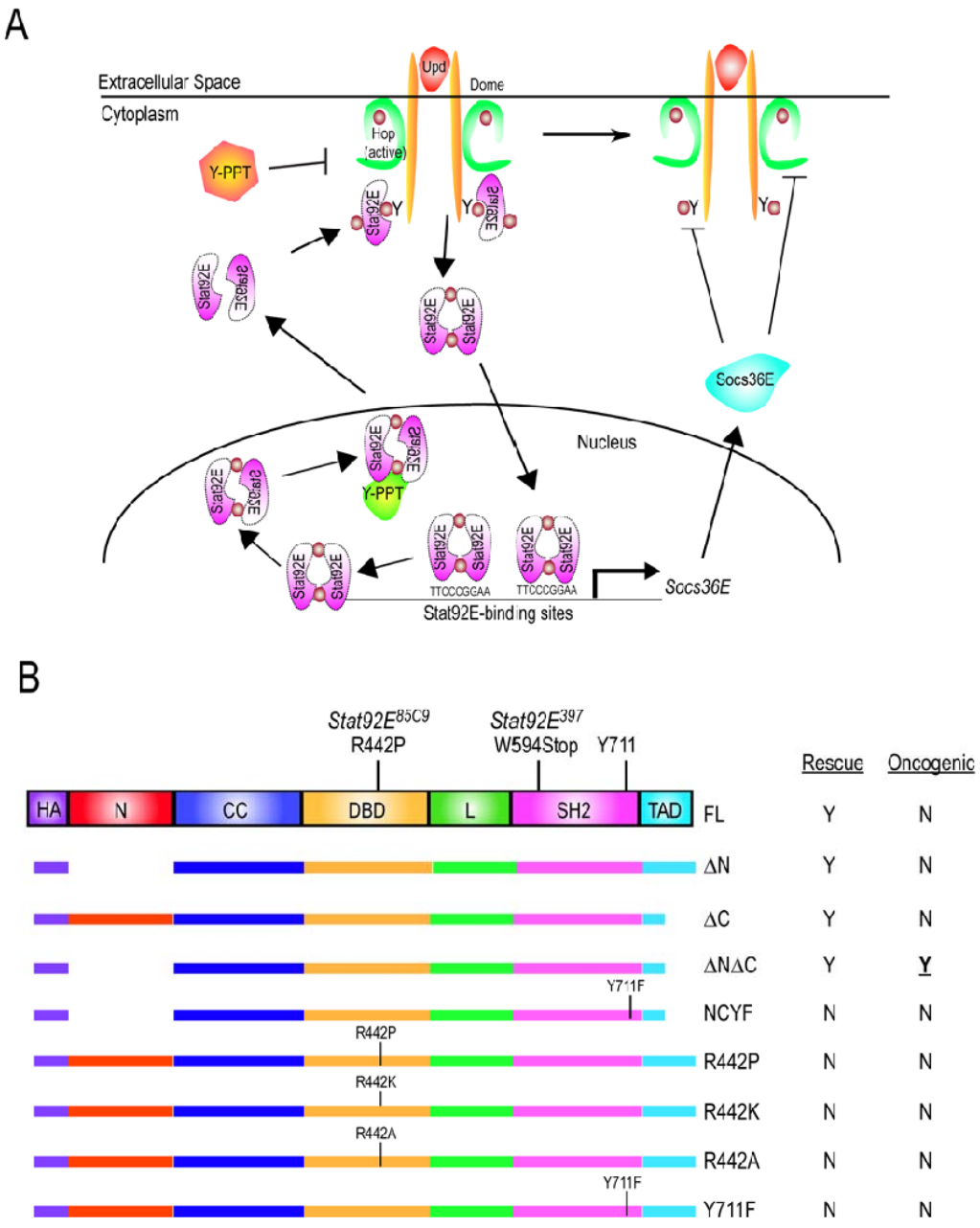

Figure 1. Model of the *Drosophila* JAK/STAT pathway and *Stat92E* transgenes

(A) Model of the *Drosophila* JAK/STAT pathway. Hop is constitutively associated with Dome and is activated by Upd binding to dimerized for of Dome (Brown et al., 2003). Activated Hop subsequently phosphorylates one or more tyrosine residues in the Dome cytoplasmic domain. Inactive, anti-parallel Stat92E dimers dock at the phospho-tyrosine residues on the receptor. Stat92E dimers are then phosphorylated by the activated Hop proteins, assume an activated dimer conformation and translocate to the nucleus where they influence the transcription of target genes. Subsequently, activated Stat92E dimers no longer bind to Stat92E binding sites on DNA; they are dephosphorylated by an unidentified nuclear tyrosine phophatase (green Y-PPT); they are then exported as unphosphorylated inactive dimers to the cytoplasm. The basal phosphorylation of Dome, Hop and/or Stat92E balanced by the actions of cytoplasmic tyrosine phosphatases (orange Y-PPT). (B) Stat92E domains

include an N-terminal (N) (red), a coiled-coil (CC) (royal blue), a DNA binding (DBD) (yellow), a linker (L) (green), an SH2 (pink), and a C-terminal trans-activation (TAD) (turquoise) domain. The critical tyrosine in Stat92E is located at residue 711. Deletions and substitutions were made to a *UAS_P-3HA-$Stat92E^{FL}$* transgene containing three N-terminal HA tags (purple). Constructs include deletion of residues 1-133 (ΔN); 725-761 (ΔC); 1-133 and 725-761 simultaneously (ΔNΔC). Substitution constructs include a mutation of the critical Y711 to F in ΔNΔC (ΔNΔCY711F); of R442 to P (R442P), R442 to K (R442K) and R442 to A (R442A); of the critical Y711 to F (Y711F). Constructs were tested in two *Stat92E* mutant backgrounds: *$Stat92E^{85C9}$*, which results from an R442P substitution, and *$Stat92E^{397}$*, which results from a premature stop at W594. “Rescue” refers to the abilty of a Stat92E variant to rescue *Stat92E* loss-of-function phenotypes *in vivo*. “Oncogenic” refers to the abilty of a Stat92E variant to cause overgrowths or melanotic tumors *in vivo*. Y = yes and N = no.

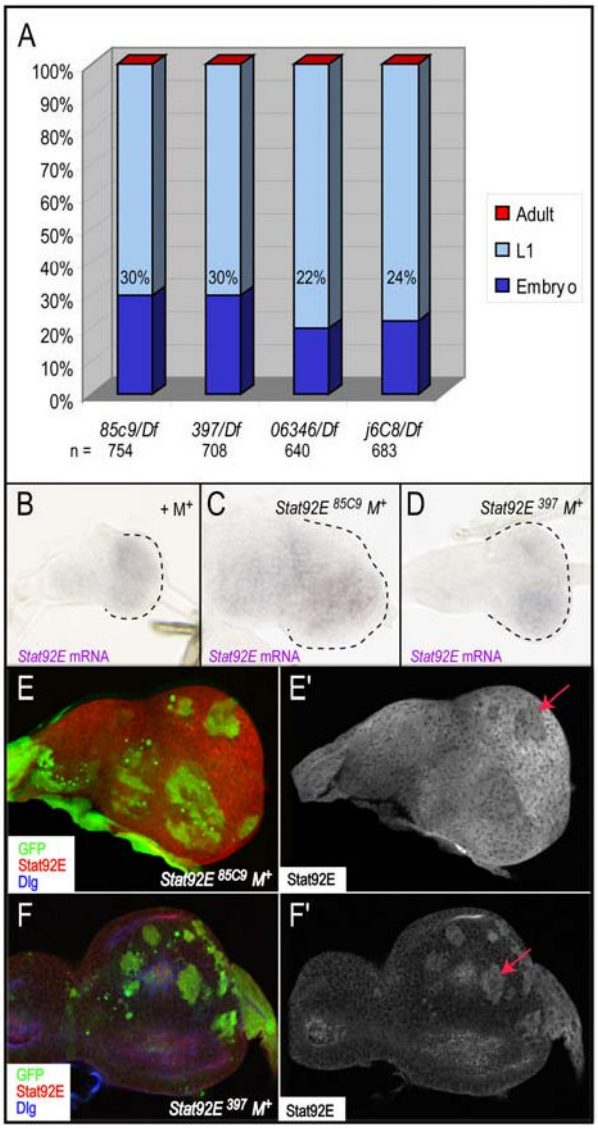

Figure 2. *Stat92E*^{85C9} and *Stat92E*^{397} are strong hypomorphic alleles

(A) Lethal phase analysis of *Stat92E*^{85C9}, *Stat92E*^{397}, *Stat92E*^{06346}, *Stat92E* ^{j6C8} alleles *in trans* to the *Df(3R)H-B79* deficiency that removes the *Stat92E* gene. Both *85C9/Df* and *397/Df* result in 30% embryonic lethality, while *06346/Df* and *j6C8/Df* result in 22% and 24%, respectively. (B-F) Large *Stat92E* clones were generated using *ey-Gal4, UAS-FLP* (*EGUF*) in a *Minute* (*M*$^{+}$) background. (A-C) *Stat92E* mRNA is produced in both *Stat92E*^{85C9} and *Stat92E*^{397} mutant backgrounds. Second instar eye discs in a control *EGUF* +*M*$^{+}$ (A), an *EGUF Stat92E*^{85C9} *M*$^{+}$ or (B), or an *EGUF Stat92E*^{397} *M*$^{+}$ background (C). (D,E) Stat92E antibody staining in *EGUF Stat92E*^{85C9}*M*$^{+}$ (H) or *EGUF Stat92E*^{397}*M*$^{+}$ (I) eye discs. *Stat92E* homozygous mutant tissue is marked by the absence of GFP (green), Stat92E is red and Dlg, which marks cell outlines, is blue. The Stat92E antibody detects Stat92E protein in *Stat92E*^{85C9} *M*$^{+}$ tissue (D). However, this antibody does not recognize antigen in *Stat92E*^{397} *M*$^{+}$ tissue because Stat92E^{397} lacks the region to which the antibody binds (last 15 amino acids of Stat92E) (E). An arrow marks GFP^{+} *Stat92E*$^{-/+}$ heterozygous tissue in D,E. For all figures, eye discs and adult eyes are oriented anterior to the left and dorsal to the top.

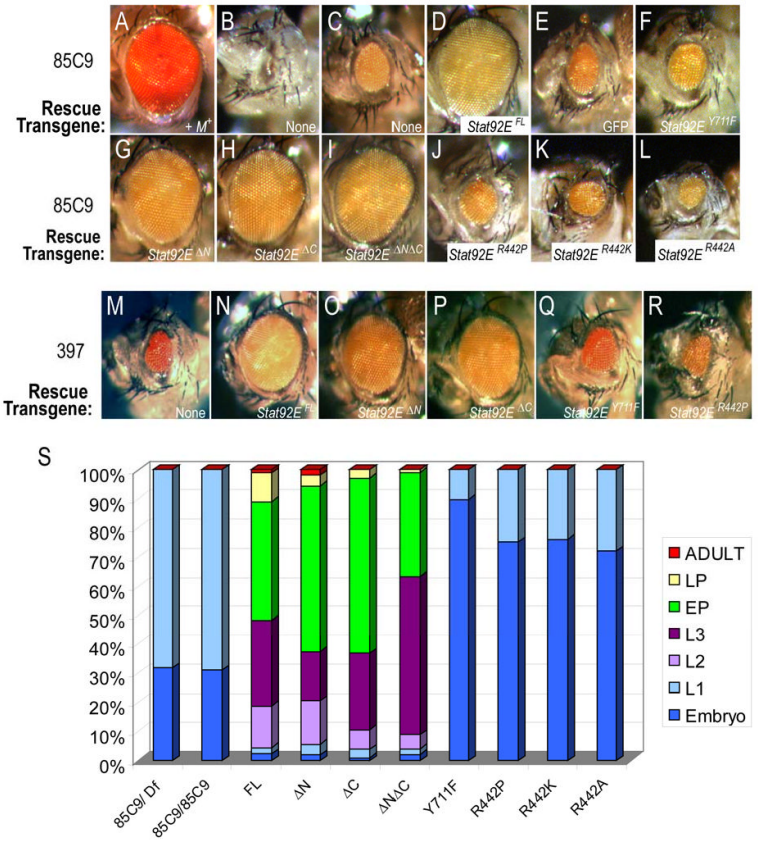

Figure 3. *Stat92E* phenotypes are rescued by Stat92E$^{\Delta N}$, Stat92E$^{\Delta C}$ and Stat92E$^{\Delta N\Delta C}$ but not by Stat92E^{Y711F} or the Stat92E^{R442} mutants

Large patches of *Stat92E* mutant tissue were generated using an *EGUF* chromosome and the *Minute* technique, where *ey-GAL4* drives *UAS-flp*, which then stimulates mitotic recombination, as well as expression of *UAS-3HA-Stat92E* rescue transgenes. (A) A +M^+ adult control eye is the same size as wild type. (B,C) *Stat92E^{85C9}* M^+ adults exhibit a no-eye (B) or small-eye (C) phenotype. (D-L) A *Stat92E^{FL}* transgene rescues the *Stat92E^{85C9}* phenotype (D), as do *Stat92E$^{\Delta N}$* (G), *Stat92E$^{\Delta C}$* (H), and *Stat92E$^{\Delta N\Delta C}$* (I). In contrast, *UAS-GFP* (E), *Stat92E^{Y711F}* (F), *Stat92E^{R442P}* (J), *Stat92E^{R442K}* (K), and *Stat92E^{R442A}* (L) do not. (M-R) *Stat92E* transgenes behave similarly when tested in *EGUF Stat92E^{397}* M^+ eye discs. (S) Lethal phase analysis of *Stat92E* variants. *Stat92E* transgenes were expressed using *tub-Gal4* in *85C9/85C9* zygotic mutants that still have maternal *Stat92E* mRNAs and the genotype *w; tub-Gal4/UAS-3HA-Stat92E; 85C9/85C9*. The FL, ΔN, ΔC, and ΔNΔC transgenes significantly delayed the *85C9/85C9* lethal phase to late pupal or infrequently adult stages. In contrast, the Y711F, R442P, R442K and R442A transgenes do not. Rather they increased the embryonic lethality in *85C9/85C9* animals. First (L1), second (L2), and third (L3) larval instar, early (EP) and late (LP) pupal stage. Animals counted: *85C9/Df*=129; *85C9/85C9*=100; *FL*=91; *ΔN*=107; *ΔC*=103; *ΔNΔC*=101; *Y711F*=194; *R442P*=157; *R442K*=160; *R442A*=111.

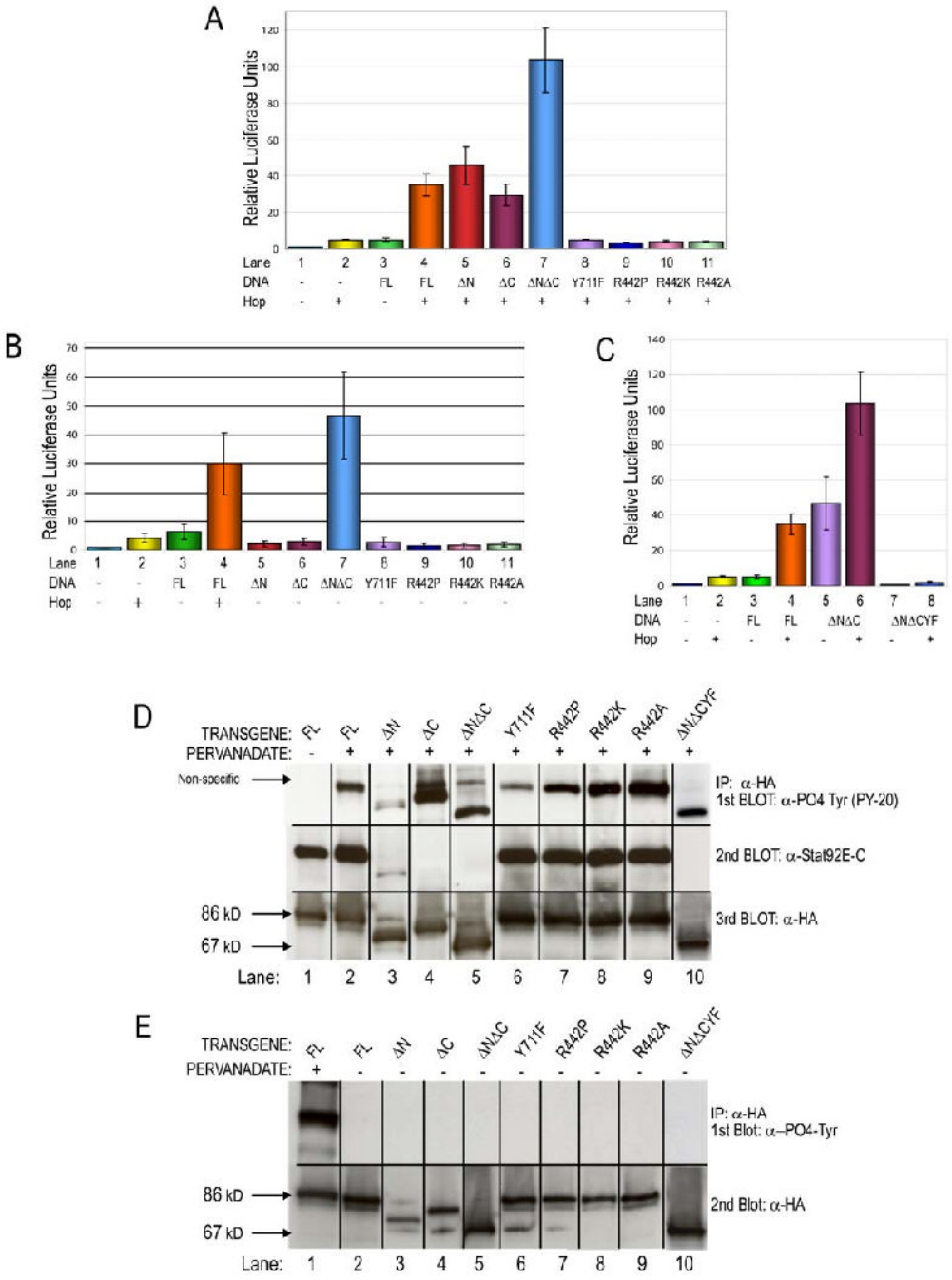

Figure 4. Transcriptional activation by and expression of Stat92E variants

(A,B) S2 cells transiently transfected with the *socs1-luc* reporter, *Ac5c-Gal4*, and *Ac5c-hop-myc-his* as noted. (A) *Ac5c-Gal4* alone, *Ac5c-hop-myc-his* alone and *Stat92E^{FL}* alone do not significantly activate *socs1-luc*. In the presence of Hop, Stat92E^{FL}, Stat92E$^{\Delta N}$, Stat92EΔC, and Stat92E$^{\Delta N\Delta C}$ activate the reporter over baseline levels. In contrast, Stat92E^{Y711F}, Stat92E^{R442P}, Stat92E^{R442K}, and Stat92E^{R442A} do not. (B) In the absence of Hop, only Stat92E$^{\Delta N\Delta C}$ activates *socs1-luc*, suggesting that it is a dominant-active mutation (lane 7). (C) The constitutive activity of Stat92E$^{\Delta N\Delta C}$ depends on phosphorylation of Y^{711}. Mutation of Tyr^{711} to Phe (Stat92E$^{\Delta N\Delta CY711F}$, abbreviated Stat92E ^{NCYF}) abolishes Stat92E$^{\Delta N\Delta C}$ activity either in the presence or absence of Hop (lanes 7 and 8). (D,E) Western blot analysis

confirms predicted expression and activation of Stat92E variants in S2 cells which were transiently transfected and stimulated as indicated. (D) In the absence of pervanadate, $Stat92E^{FL}$ is expressed but not tyrosine phosphorylated (lane 1). In contrast, all Stat92E variants are phosphorylated in response to pervanadate treatment (lanes 2-10). Reprobing the blot with C-terminal Stat92E specific or HA specific antibodies reveals that all Stat92E variants are expressed at their predicted M_r. $Stat92E^{\Delta C}$, $Stat92E^{\Delta N \Delta C}$ and $Stat92E^{NCYF}$ (lanes 4,5 and 10) are not detected by the Stat92E antibody because antigen recognized by this antibody. (E) None of the Stat92E variants are tyrosine phosphorylated in the absence of pervanadate (lanes 2-10). Activation of $Stat92E^{FL}$ by pervanadate (lane 1) serves as a positive control for tyrosine phosphorylation.

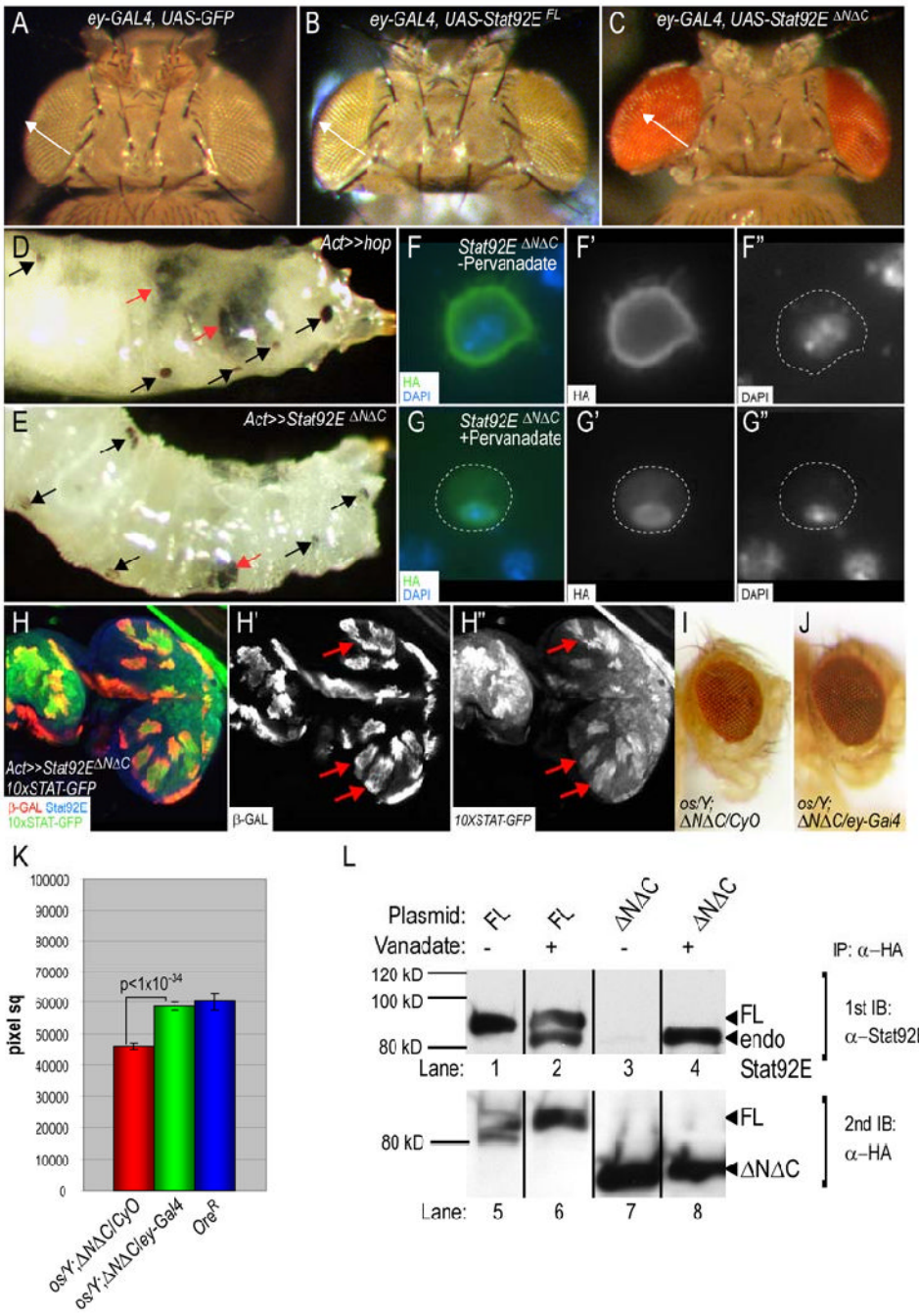

Figure 5. Stat92E$^{\Delta N\Delta C}$ exhibits constitutive activity

(A-C) Dorsal view of adult heads from animals in which *ey-Gal4* (Hauck et al., 1999) drives expression of *UAS-GFP* (A), of *UAS-Stat92E^{FL}* (B) or of *UAS-Stat92E$^{\Delta N\Delta C}$* (C) during larval eye development. Arrow (white) denotes the distance from the medial posterior to the anterior lateral edge of the eye. This standard was used to demonstrate that ectopic expression of *Stat92E$^{\Delta N\Delta C}$* (C) but not *Stat92E^{FL}* (B) leads to eye overgrowth. (D,E) Third instar larvae with randomly induced clones expressing Hop (*Act≫hop*) (D) or Stat92E$^{\Delta N\Delta C}$ (*Act≫Stat92E$^{\Delta N\Delta C}$*) have melanotic tumors (large tumors, red arrows; small tumors, black arrows in D,E). (F,G) Stat92E$^{\Delta N\Delta C}$ is not constitutively localized to the nucleus. S2 cells expressing Stat92E$^{\Delta N\Delta C}$ were unstimulated (F) or stimulated with pervanadate (G). HA

(green), DAPI (blue). In the absence of stimulation, Stat92E$^{\Delta N \Delta C}$ is cytoplasmic (F), but moves into the nucleus upon activation (G). (H) A third instar eye disc harboring *Stat92E$^{\Delta N \Delta C}$*-expressing-clones (*Act≫Stat92E$^{\Delta N \Delta C}$*) and the *10×STAT-GFP* reporter. Clones (anti-β GAL (red)), *10×STAT-GFP* (green), anti-Stat92E-C (blue). Ectopic expression of *Stat92E$^{\Delta N \Delta C}$* induces the expression of the Stat92E transcriptional reporter *10×STAT-GFP* in a cell-autonomous manner (red arrows). (I-J) Stat92E$^{\Delta N \Delta C}$ acts downstream of *upd*. An *os/Y; UAS-Stat92E$^{\Delta N \Delta C}$/CyO* male has small eyes (I). This phenotype was rescued in *os/Y; UAS-Stat92E$^{\Delta N \Delta C}$/ey-Gal4* flies, where Stat92E$^{\Delta N \Delta C}$ is specifically expressed in the eye disc (J). (K) Quantification of the eye area in *os/Y; UAS-3HA-Stat92E$^{\Delta N \Delta C}$/CyO* (red bar), *os/Y; UAS-3HA-Stat92Ei$^{N \Delta C}$/CyO* (green bar) or wild type +/*Y* males (blue bar). 80=eyes in each *os/Y* genotype. n=20 in wild type. The difference between the values of the red and green values is statistically significant ($p<10^{-34}$, Student's T test). (L) Stat92E^{FL} and Stat92E$^{\Delta N \Delta C}$ dimerize with endogenous Stat92E. S2 cells were transiently transfected with the indicated plasmids and were unstimulated or treated with pervanadate. 3HA-Stat92E proteins were immunoprecicipated with an HA antibody and Western blotted first with Stat92E-C and subsequently HA antibodies. Endogenous Stat92E has a predicted M_r of 85 kDa (lanes 2,4), the 3HA-Stat92E^{FL} protein 90 kDa (lane 1) and 3HA-Stat92E$^{\Delta N \Delta C}$ 67 kDa (lane 3). Endogenous Stat92E does not co-immunoprecipitate with either variant in the absence of pervanadate (lanes 1 and 3). However, after activation of the pathway, endogenous Stat92E present in anti-HA precipitates (lanes 2 and 4).

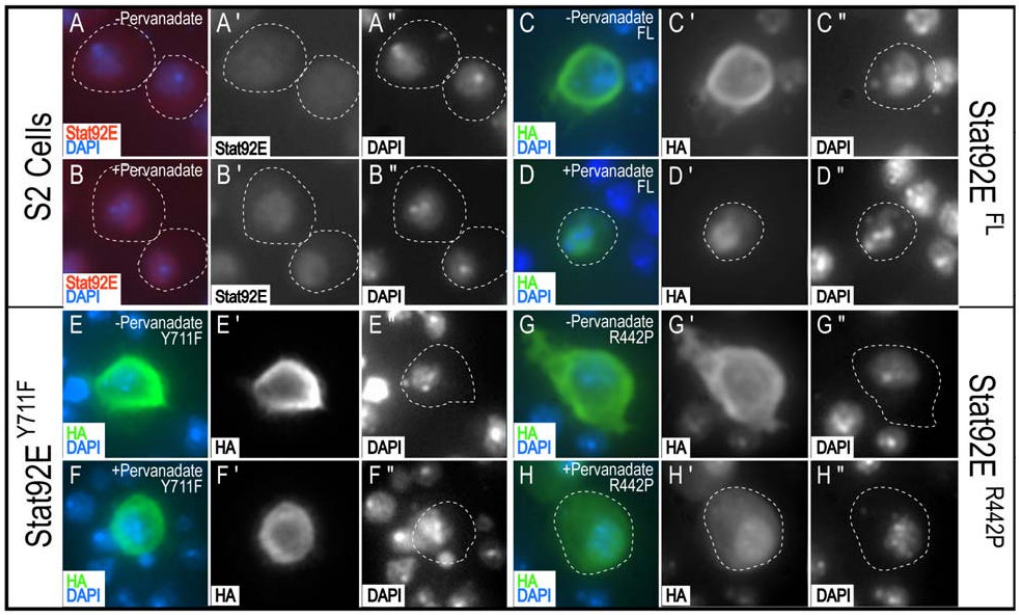

Figure 6. Stat92E^{R442P} can translocate to the nucleus after activation

Untransfected S2 cells (A,B), or S2 cells transiently transfected with *Stat92E^{FL}* (C,D), *Stat92E^{Y711F}* (E,F), or *Stat92E^{R442P}*(G,H). Cells were unstimulated (A,C,E,G) or stimulated with pervanadate (B,D,F,H). Stat92E (red), HA (green), and DAPI (blue). In the absence of stimulation, endogenous Stat92E (A), Stat92E^{FL} (C), Stat92E^{Y711F} (E), and Stat92E^{R442P} (G) are cytoplasmic. Upon stimulation, endogenous Stat92E (B), Stat92E^{FL} (D) and Stat92E^{R442P} (H) translocate to the nucleus. Stat92E^{Y711F} (F) does not translocate to the nucleus upon stimulation.

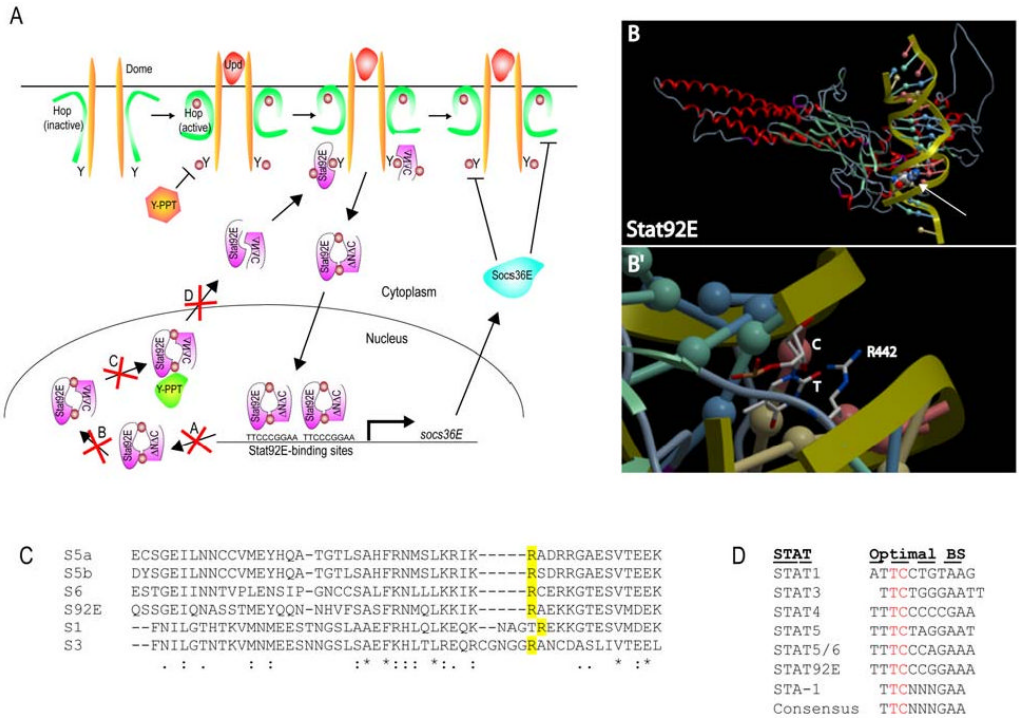

C

S5a	ECSGEILNNCCVMEYHQA-TGTLSAHFRNMSLKRIK-----RADRRGAESVTEEK
S5b	DYSGEILNNCCVMEYHQA-TGTLSAHFRNMSLKRIK-----RSDRRGAESVTEEK
S6	ESTGEIINNTVPLENSIP-GNCCSALFKNLLLKKIK-----RCERKGTESVTEEK
S92E	QSSGEIQNASSTMEYQQN-NHVFSASFRNMQLKKIK-----RAEKKGTESVMDEK
S1	--FNILGTHTKVMNMEESTNGSLAAEFRHLQLKEQK--NAGTREKKGTESVMDEK
S3	--FNILGTNTKVMNMEESNNGSLSAEFKHLTLREQRCGNGGRANCDASLIVTEEL

D

STAT	Optimal BS
STAT1	ATTCCTGTAAG
STAT3	TTCTGGGAATT
STAT4	TTTCCCCCGAA
STAT5	TTTCTAGGAAT
STAT5/6	TTTCCCAGAAA
STAT92E	TTTCCCGGAAA
STA-1	TTCNNNGAA
Consensus	TTCNNNGAA

Figure 7. Model of action of Stat92E$^{\Delta N \Delta C}$ and of Stat92E^{R442}

(A) Basal levels of tyrosine phosphorylation of Dome, Hop and/or Stat92E are kept in check by cellular tyrosine phosphatases (orange Y-PPT). Inactive Stat92E^{FL}:Stat92E$^{\Delta N \Delta C}$ dimers exist at low levels in the cytoplasm of unstimulated cells and can bind to the basally-actiavted phosphorylated receptor via their intact SH2 domains. Once bound to the activated receptor, these Stat92E proteins are themselves phosphorylated, leading to the formation of activated Stat92E^{FL}:Stat92E$^{\Delta N \Delta C}$ dimers that translocate to the nucleus, bind consensus Stat92E binding elements on DNA and modulate gene transcription. Possible molecular mechanism underlying the dominant active behavior of the Stat92E^{FL}:Stat92E$^{\Delta N \Delta C}$ dimers. They could (A) stay bound longer to DNA that endogenous dimers; (B) be more resistant to conformational change to an unphosphorylated dimer; (C) be more resistant to dephosphorylation by a nuclear tyrosine phosphatase (green Y-PPT) and/or (D) resist export from the nucleus. (B) Homology model of Stat92E based on the crystallographic structure of a phosphorylated STAT1 dimer bound to DNA (Chen et al., 1998). Arg^{442} is displayed as spherical space-filled atoms and contacts DNA in the minor groove (white arrow). (B′) Zoom of (A). Arg^{442} is shown in stick figure form. Arg^{442} appears to be interacting with a thymine (T, shown in stick figure form) and with a cytosine (C, shown as a red ball) located in the minor groove of the DNA helix. (D) The optimal DNA binding sites for mammalian STATs 1-6, Stat92E and STA-1.